fractal and fractional

MDPI

Article

Dynamics of a Delayed Fractional-Order Predator–Prey Model with Cannibalism and Disease in Prey

Hui Zhang [1,2] and Ahmadjan Muhammadhaji [1,2,*]

[1] College of Mathematics and System Sciences, Xinjiang University, Urumqi 830017, China; 107552200593@stu.xju.edu.cn
[2] Xinjiang Key Laboratory of Applied Mathematics, Xinjiang University, Urumqi 830017, China
* Correspondence: ahmatjanam@aliyun.com

Abstract: In this study, a class of delayed fractional-order predation models with disease and cannibalism in the prey was studied. In addition, we considered the prey stage structure and the refuge effect. A Holling type-II functional response function was used to describe predator–prey interactions. First, the existence and uniform boundedness of the solutions of the systems without delay were proven. The local stability of the equilibrium point was also analyzed. Second, we used the digestion delay of predators as a bifurcation parameter to determine the conditions under which Hopf bifurcation occurs. Finally, a numerical simulation was performed to validate the obtained results. Numerical simulations have shown that cannibalism contributes to the elimination of disease in diseased prey populations. In addition, the size of the bifurcation point τ_0 decreased with an increase in the fractional order, and this had a significant effect on the stability of the system.

Keywords: cannibalism; disease; fractional order; stability; Hopf bifurcation

check for updates

Citation: Zhang, H.; Muhammadhaji, A. Dynamics of a Delayed Fractional-Order Predator–Prey Model with Cannibalism and Disease in Prey. *Fractal Fract.* **2024**, *8*, 333. https://doi.org/10.3390/fractalfract8060333

Academic Editor: Carlo Cattani

Received: 16 April 2024
Revised: 23 May 2024
Accepted: 30 May 2024
Published: 3 June 2024

1. Introduction

There are different types of species relationships, including cooperation, competition, and predation, among which predation relationships have always been a concern [1–3]. Models of stage structure in populations have proven useful in many different systems, as highlighted in previous research [4]. In a simple predator–prey (PP) system, both predators and prey develop in stages, leading to variations in physiological and behavioral characteristics among species at different stages. Understanding the biological and ecological dimensions of a species is crucial because the growth of all species is a dynamic process that involves various stages. The stage structure of populations is fundamental to ecology, and studies have demonstrated that models exploring this structure are valuable across various systems [4]. For many organisms, stage is a more accurate predictor of demographic rate than age [5]. Consequently, the consideration of stage structures in predation models has sparked significant interest among mathematicians and ecologists [6–8].

In nature, every species naturally interacts with others, and PP interactions are often characterized by functional responses [9]. A variety of functional response functions have been used to describe species interactions. One commonly employed function in PP systems is the Holling type-II response function [10,11], which provides a comprehensive understanding of the pressure that predators exert on prey populations, making it integral in the study of PP interactions in ecosystems. Another vital aspect when studying PP systems is the prey refuge [12,13]. Prey refuges can be broadly defined as strategies or environments that reduce predation risks [14]. By employing these safeguards, prey can effectively avoid being eaten and weaken predator populations to an extent. An excellent example is the role of seaweed in marine ecosystems. Seaweed acts as a protective shelter, allowing small fish and crustaceans to effectively hide from oceanic predators. Consequently, these predators face challenges when directly hunting

prey because of the protective environments provided by seaweed. Such refuges offered by seaweed significantly contribute to the maintenance of biodiversity and the ecological balance within marine ecosystems. Understanding the significance of prey refuges and their effects on PP interactions is crucial for ecological research and conservation. This refuge illustrates the intricate and interconnected nature of species interactions in natural ecosystems.

Cannibalism is frequently observed in animal populations [15,16]. Ecologists are intrigued by the reasons behind cannibalism and its persistence, and extensive research has been conducted in this area [17–19]. Remarkably, in [17], the authors point out the lack of studies in the ecological and evolutionary literature regarding the impact of cannibalism on parasites and its implications for the relationship between cannibalism and disease. Therefore, when considering the feedback between parasites and cannibalism, some experiments have concluded that cannibalism may be more likely to reduce the prevalence of parasites and thus limit their negative effects on cannibalistic behavior. Mathematicians have also paid close attention to the study of cannibalism among populations. Based on this, many related mathematical models have been established [20–22]. In particular, the effects of cannibalism and disease on population dynamics are considered. For example, Li et al. [23] studied the bifurcation control problem of a class of delay fractional-order PP systems with cannibalism and diseases. In [24], the authors proposed and analyzed a PP model of cannibalism with infectious diseases in a predator population. Hopf bifurcation and local stability analyses of the system near the bioviable equilibrium point were performed. Cannibalistic interactions between different developmental stages are prevalent in many animal and social insect species. For example, when there is a high density of juveniles, some adults may consume the offspring to increase survival and reproductive success. In particular, when some young populations are infected with diseases, mature individuals consider consuming these disease-carrying young individuals to ensure the survival of offspring with a higher survival and reproductive potential. In addition, in [25–27], the authors investigated the bifurcation behavior and stability of the considered PP system with a stage structure or cannibalism. However, these studies did not consider the stage structure of the species in terms of cannibalism and disease.

Recently, fractional calculus has continually advanced, with fractional differential equations finding extensive applications in fields such as astrophysics, economics, and chemistry [28–30]. Many excellent results have been reported, particularly in the field of cybernetics [31,32]. There is a close relationship between the fractional derivative and memory, which can reflect the "memory dependence" of some dynamic processes to a certain extent. This is one advantage of fractional derivatives over integer derivatives. Long-term memory effects have also been observed in many populations [33,34]. For example, Zhou et al. [33] show that organisms can retain information about temporal environmental stimuli as "stress memories". Stressor-induced memories can benefit organisms when exposed to stressors that are later triggered. Therefore, the application of fractional derivatives is of practical significance [10,35–38].

Inspired by the aforementioned article, this study focused on a delayed fractional predation model of cannibalism and disease. For the first time, we have linked disease, cannibalism, and stage structure. Adult prey are usually highly immune to disease, and pandemics occur only in young prey; mature prey selectively eat sick young individuals to promote better survival of their offspring. In addition, the Holling type-II functional response was used to describe the interaction between prey and predators and to consider the protection of prey in shelters.

The structure of this paper is as follows: Section 2 discusses some preparatory knowledge related to the fractional order. The mathematical model is presented in Section 3. In Section 4, we examine the existence and boundedness of solutions for systems without delay. Section 5 describes the local stability at each equilibrium point. In Section 6, the Hopf bifurcation caused by time delay is discussed. Section 7 discusses

relevant numerical simulations. Finally, the paper is summarized and conclusions are presented.

2. Preliminaries

In this section, we first introduce the definition and fundamental properties of the Caputo derivative, which will be referenced later in this article.

Definition 1 ([39]). *Function $f(t)$ is said to be a Caputo fractional derivative if there is a positive constant $n-1<\varrho<n$, $n\in Z^+$ such that*

$$^cD^{\varrho}f(t)=\frac{1}{\Gamma(n-\varrho)}\int_0^t(t-\tau)^{n-\varrho-1}f^n(\tau)d\tau,$$

where $\Gamma(\cdot)$ is the Gamma function.

The following is the Laplace transform of the Caputo fractional-order derivative:

$$\pounds\{^cD^{\varrho}f(t);s\}=s^{\varrho}F(s)-\sum_{i=1}^{n-1}s^{\varrho-i-1}f^{(i)}(0),$$

where $F(s)=\pounds\{f(t)\}$. In particular, when $f^{(i)}(0)=0, i=1,2,\ldots,n-1$, then $\pounds\{^cD^{\varrho}f(t);s\}=s^{\varrho}F(s)$.

Theorem 1 ([40]). *For each $c>0, d>0$ and $K\in C^{n\times n}$, we get*

$$\pounds\left\{t^{d-1}E_{c,d}(Kt^c)\right\}=\frac{p^{c-d}}{p^c-K},$$

for $\mathcal{R}(p)>\|K\|^{\frac{1}{c}}$, where $\mathcal{R}(p)$ stands for the real part of the complex number p, and $E_{c,d}$ is the Mittag–Leffler function defined as $E_{c,d}(z)=\sum_{n=0}^{\infty}\frac{z^c}{\Gamma(cn+d)}$.

Theorem 2 ([41]). *Consider the following fractional-order system:*

$$^cD^{\varrho}x(t)=f(x),\quad x(0)=x_0, \tag{1}$$

with $\varrho\in(0,1)$ and $x\in R^n$. The equilibrium points of the above system are the solutions of $f(x)=0$. An equilibrium is locally asymptotically stable if all eigenvalues λ_j of the Jacobian matrix $J=\frac{\partial f}{\partial x}$ evaluated at the equilibrium satisfy $|\arg(\lambda_i)|>\frac{\varrho\pi}{2}$.

3. The Model

In [23], the authors discussed the following delayed fractional-order PP model with cannibalism and disease:

$$\begin{aligned}
^cD^{\varrho}x(t)=&x(t)(1-x(t))-\frac{a_1x(t)y(t)}{a_2+x(t)},\\
^cD^{\varrho}y(t)=&ry(t)\left[1-\frac{h(y(t-\tau)+z(t-\tau))}{x(t-\tau)}\right]-\frac{b_1y(t)z(t)}{b_2+y(t)}-\sigma_1y^2(t)\\
&+c_2\sigma_2y(t)z(t)+c_1\sigma_1y^2(t)-d_1y(t),\\
^cD^{\varrho}z(t)=&\frac{b_1y(t)z(t)}{b_2+y(t)}-\sigma_2y(t)z(t)-d_2z(t),
\end{aligned} \tag{2}$$

where $x(t)$ is the density of the prey, $y(t)$ is the density of the susceptible predator, and $z(t)$ is the density of the infected predator. In [23], the authors obtained the asymptotic properties and Hopf bifurcation of system (2). In [25], Huang et al. considered a delayed fractional-order PP system:

$$
\begin{aligned}
{}^{c}D^{\varrho_1}x(t) =& x(t)\left[r - ax(t-\delta) - \frac{a_1 x(t) y_2(t)}{m y_2^2(t) + x^2(t)}\right], \\
{}^{c}D^{\varrho_2}y_1(t) =& \frac{a_2 x^2(t-\delta) y_2(t-\delta)}{m y_2^2(t-\delta) + x^2(t-\delta)} - r_1 y_1(t) - D y_1(t), \\
{}^{c}D^{\varrho_3}y_2(t) =& D y_1(t) - r_2 y_2(t),
\end{aligned} \tag{3}
$$

where $x(t)$ stands for the density of the prey population at time t and $y_1(t)$ and $y_2(t)$ denote the densities of the immature and the mature predator population at time t, respectively. The author focused on the study of the predator's stage structure and studied the bifurcation control of system (3).

Inspired by the above analysis and works, firstly, we propose a novel PP model with cannibalism and disease in prey. The specific model is as follows:

$$
\begin{aligned}
{}^{c}D^{\varrho}x_1^s(t) &= \alpha x_2(t) - \Omega x_1^s(t) - \theta x_1^s(t) x_1^i(t) - d x_1^s(t), \\
{}^{c}D^{\varrho}x_1^i(t) &= \theta x_1^s(t) x_1^i(t) - \varphi x_2(t) x_1^i(t) - d_1 x_1^i(t), \\
{}^{c}D^{\varrho}x_2(t) &= \Omega x_1^s(t) - \frac{\mu(1-m) x_2(t) y(t)}{1 + a(1-m)x_2(t)} + c\varphi x_2(t) x_1^i(t) - \eta x_2^2(t) - d_2 x_2(t), \\
{}^{c}D^{\varrho}y_3(t) &= \frac{e\mu(1-m) x_2(t-\tau) y(t-\tau)}{1 + a(1-m)x_2(t-\tau)} - d_3 y(t),
\end{aligned} \tag{4}
$$

where the density of the susceptible immature prey is $x_1^s(t)$, the density of the infected immature prey is $x_1^i(t)$, the density of the mature prey is $x_2(t)$, and the density of the predator is $y(t)$. In addition, $mx_2(t)$ can protect the prey in a more secure area $(0 < m < 1)$. Thus, $(1-m)x_2(t)$ of the mature prey is consumed by the predator.

In order to derive our model, we suppose the following:

(i) The disease is only transmitted between the immature prey populations;

(ii) The infected immature prey will not recover from the disease, and this portion of the infected immature prey can not normally grow into mature prey populations;

(iii) During cannibalism, the disease will not spread.

The meanings of the parameters of system (4) are shown in Table 1. All the parameters are assumed as positive constants.

Table 1. Biological meaning of the parameters in system (4).

Parameter	Description
α	The birth rate of juvenile prey.
Ω	The transition from uninfected immature prey to mature prey.
θ	The transmission rate of the disease among immature prey.
φ	Predation rate of mature prey on infected immature prey.
c	The conversion rate of immature prey to mature prey due to cannibalism.
η	The coefficient of competition between mature prey.
μ	Predation rate of the predator to mature prey.
e	The conversion rate of predation from mature prey to predator.
m	The prey refuge rate.
a	Half saturation constants.
d	The death rate of susceptible immature prey.
d_1	The death rate of infected immature prey.
d_2	The death rate of mature prey.
d_3	The death rate of predators.
τ	The time delay generated by predation and digestion.

It is worth noting that using the Holling type-II functional response function in system (4) to describe the interaction between predators and prey has a kind of reasonable biological interpretation. In fact, simply describing the interaction between predators and prey with a linear relationship does not conform to the actual situation. Under certain circumstances, the increase in the number of prey will lead to an increase in the feeding rate of the predator, because there are more prey available for predation. With the increase in the feeding rate, the number of prey begins to decrease, which in turn limits the feeding rate of the predator. This negative feedback loop can maintain the relative stability between the predator and the prey. Many scholars have already applied the Holling type-II functional response function to the predation system [10,11,42].

Next, to make the model more concise, let $\beta = d + \Omega$, $\psi = c\varphi, \sigma = e\mu$. Hence, system (4) transforms to:

$$\begin{aligned}
{}^{c}D^{\varrho}x_1^s(t) &= \alpha x_2(t) - \beta x_1^s(t) - \theta x_1^s(t)x_1^i(t),\\
{}^{c}D^{\varrho}x_1^i(t) &= \theta x_1^s(t)x_1^i(t) - \varphi x_2(t)x_1^i(t) - d_1 x_1^i(t),\\
{}^{c}D^{\varrho}x_2(t) &= \Omega x_1^s(t) - \frac{\mu(1-m)x_2(t)y(t)}{1+a(1-m)x_2(t)} + \psi x_2(t)x_1^i(t) - \eta x_2^2(t) - d_2 x_2(t),\\
{}^{c}D^{\varrho}y_3(t) &= \frac{\sigma(1-m)x_2(t-\tau)y(t-\tau)}{1+a(1-m)x_2(t-\tau)} - d_3 y(t),
\end{aligned} \tag{5}$$

with initial conditions

$$x_1^s(0) > 0, x_1^i(0) > 0, x_2(0) > 0, y(0) > 0. \tag{6}$$

4. Existence and Boundness

In this section, for $\tau = 0$, we will study some properties of system (5).

Theorem 3. *System (5) has a unique solution for all the nonnegative initial conditions.*

Proof. In order to prove the theorem, we consider a region $\Psi \times (t_0, T)$, $T < \infty$, where $\Psi = \{(x_1^s, x_1^i, x_2, y) \in R^4,\ \max(|x_1^s|, |x_1^i|, |x_2|, |y|) = M\}$. Then, we consider a map

$$F(X) = (F_1(X), F_2(X), F_3(X), F_4(X)),$$

where $X = (x_1^s, x_1^i, x_2, y)$ and $\widehat{X} = (\widehat{x_1^s}, \widehat{x_1^i}, \widehat{x_2}, \widehat{y})$,

$$\begin{aligned}
F_1(X) &= \alpha x_2(t) - \beta x_1^s(t) - \theta x_1^s(t)x_1^i(t),\\
F_2(X) &= \theta x_1^s(t)x_1^i(t) - \varphi x_2(t)x_1^i(t) - d_1 x_1^i(t),\\
F_3(X) &= \Omega x_1^s(t) - \frac{\mu(1-m)x_2(t)y(t)}{1+a(1-m)x_2(t)} + \psi x_2(t)x_1^i(t) - \eta x_2^2(t) - d_2 x_2(t),\\
F_4(X) &= \frac{\sigma(1-m)x_2(t)y(t)}{1+a(1-m)x_2(t)} - d_3 y(t).
\end{aligned}$$

For any $X, \widehat{X} \in \Psi$, we have

$$
\begin{aligned}
&\|F(X)-F(\widehat{X})\| \\
=&\sum_{i=1}^{4}|F_i(X)-F_i(\widehat{X})| \\
=&\mid \alpha x_2-\beta x_1^s-\theta x_1^s x_1^i-[\alpha\widehat{x}_2-\beta\widehat{x}_1^s-\theta\widehat{x}_1^s\widehat{x}_1^i]\mid \\
&+\mid \theta x_1^s x_1^i-\varphi x_2 x_1^i-d_1x_1^i-[\theta\widehat{x}_1^s\widehat{x}_1^i-\varphi\widehat{x}_2\widehat{x}_1^i-d_1\widehat{x}_1^i]\mid \\
&+\mid \Omega x_1^s-\frac{\mu(1-m)x_2y}{1+a(1-m)x_2}+\psi x_2x_1^i-\eta x_2^2-d_2\,x_2 \\
&-[\Omega\widehat{x}_1^s-\frac{\mu(1-m)\widehat{x}_2\widehat{y}}{1+a(1-m)\widehat{x}_2}+\psi\widehat{x}_2\widehat{x}_1^i-\eta\widehat{x}_2^2-d_2\widehat{x}_2]\mid \\
&+\mid \frac{\sigma(1-m)x_2y}{1+a(1-m)x_2}-d_3y-[\frac{\sigma(1-m)\widehat{x}_2\widehat{y}}{1+a(1-m)\widehat{x}_2}-d_3\widehat{y}]\mid \\
\le&\{\beta+2\theta M+\Omega\}\mid x_1^s-\widehat{x}_1^s\mid+\{(2\theta+\varphi+\psi)M+d_1\}\mid x_1^i-\widehat{x}_1^i\mid \\
&+\{(\alpha+\varphi+\psi+2\eta)M+d_2+\frac{\mu(1-m)M+2M^2a(1-m)}{(1+a(1-m))^2} \\
&+\frac{\sigma(1-m)M+2M^2a(1-m)}{(1+a(1-m))^2}\}\mid x_2-\widehat{x}_2\mid+\{\frac{\mu(1-m)M+M^2a(1-m)}{(1+a(1-m))^2} \\
&+\frac{\sigma(1-m)M+M^2a(1-m)}{(1+a(1-m))^2}+d_3\}\mid y-\widehat{y}\mid \\
\le&\ell|F(X)-F(\widehat{X})\|.
\end{aligned}
$$

where

$$
\begin{aligned}
\ell=&\max\{\beta+2\theta M+\Omega,(2\theta+\varphi+\psi)M+d_1,(\alpha+\varphi+\psi+2\eta)M+d_2+ \\
&\frac{(\mu+\sigma)(1-m)M+4M^2a(1-m)}{(1+a(1-m))^2},\frac{(\mu+\sigma)(1-m)M+2M^2a(1-m)}{(1+a(1-m))^2}+d_3\}.
\end{aligned}
$$

Thus, F satisfies the local Lipschitz condition, which implies the theorem is proven. □

Theorem 4. *All the solutions of system (5) are uniformly bounded in the domain* Ψ*, where*

$$
\Psi=\left\{(x_1^s,x_1^i,x_2,y)\in R_+^4\mid 0<x_1^s(t)+x_1^i(t)+x_2(t)+y(t)\le\frac{\alpha^2}{4\eta\Upsilon}+\delta,\delta>0\right\}.
$$

Proof. Define the function

$$
\aleph=x_1^s(t)+x_1^i(t)+x_2(t)+y(t). \tag{7}
$$

Then, applying the Caputo fractional derivative to (7) yields

$$
\begin{aligned}
{}^cD^\varrho\aleph(t)=&{}^cD^\varrho x_1^s(t)+{}^cD^\varrho x_1^i(t)+{}^cD^\varrho x_2(t)+{}^cD^\varrho y(t) \\
=&\alpha x_2(t)-\beta x_1^s(t)-\theta x_1^s(t)x_1^i(t)+\theta x_1^s(t)x_1^i(t)-\varphi x_2(t)x_1^i(t)-d_1x_1^i(t) \\
&+\Omega x_1^s(t)-d_3y(t)-\frac{\mu(1-m)x_2(t)y(t)}{1+a(1-m)x_2(t)}+\frac{\sigma(1-m)x_2(t)y(t)}{1+a(1-m)x_2(t)} \\
&-\eta x_2^2(t)-d_2x_2(t)+\psi x_2(t)x_1^i(t) \\
\le&\alpha x_2(t)-dx_1^s(t)-d_1x_1^i(t)-d_2x_2(t)-d_3y(t)-\eta x_2^2(t).
\end{aligned} \tag{8}
$$

If $\Lambda = \min\{d, d_1, d_2, d_3\}$, then the following formula is valid:

$$^{c}D^{\varrho}\aleph(t) + \Lambda\aleph(t) \leq -\eta(z_2(t) - \frac{\alpha}{2\eta})^2 + \frac{\alpha^2}{4\eta} \leq \frac{\alpha^2}{4\eta}. \tag{9}$$

By applying the Laplace transform to (9), it holds that

$$s^{\varrho}F(s) - s^{\varrho-1}\aleph(0) + \Upsilon F(s) \leq \frac{\alpha^2}{4\eta s}. \tag{10}$$

where $F(s) = \pounds\{\aleph(t)\}$. Multiply both sides of the (10) by s.

$$\left[s^{\varrho+1} + \Upsilon s\right]F(s) \leq s^{\varrho}\aleph(0) + G, \tag{11}$$

where $G = \frac{\alpha^2}{4\eta}$. Based on (11), we have

$$F(s) \leq \aleph(0)\frac{s^{-1}}{s^{\varrho} + \Upsilon} + \frac{G}{s(s^{\varrho} + \Upsilon)}. \tag{12}$$

Taking the inverse Laplace transform of both sides of (12), we get

$$\aleph(t) \leq \aleph(0)\pounds^{-1}\left\{\frac{s^{\varrho-1}}{s^{\varrho} + \Upsilon}\right\} + G\pounds^{-1}\left\{\frac{s^{\varrho-(\varrho+1)}}{s^{\varrho} + \Upsilon}\right\}. \tag{13}$$

Using Theorem 1, we can obtain

$$\aleph(t) \leq \aleph(0)E_{\varrho,1}\{-\Upsilon t^{\varrho}\} + Gt^{\varrho}E_{\varrho,\varrho+1}\{-\Upsilon t^{\varrho}\}. \tag{14}$$

By the properties of the Mittag–Leffler function, we have

$$E_{\varrho,1}\{-\Upsilon t^{\varrho}\} = (-\Upsilon t^{\varrho})E_{\varrho,\varrho+1}\{-\Upsilon t^{\varrho}\} + \frac{1}{\Gamma(1)}, \tag{15}$$

that is to say

$$t^{\varrho}E_{\varrho,\varrho+1}\{-\Upsilon t^{\varrho}\} = -\frac{1}{\Upsilon}\left[E_{\varrho,1}\{-\Upsilon t^{\varrho}\} - 1\right]. \tag{16}$$

Therefore,

$$\aleph(t) \leq \left\{\aleph(0) - \frac{G}{\Upsilon}\right\}E_{\varrho,1}\{-\Upsilon t^{\varrho}\} + \frac{G}{\Upsilon}. \tag{17}$$

Since $E_{\varrho,1} \to 0$ ($t \to \infty$), all the solutions of system (5) are uniformly bounded in the region

$$\Psi = \left\{(x_1^s, x_1^i, x_2, y) \in R_+^4 \mid 0 < x_1^s(t) + x_1^i(t) + x_2 + y(t) \leq \frac{\alpha^2}{4\eta\Upsilon} + \delta, \delta > 0\right\}.$$

This completes the proof of Theorem 4. □

Remark 1. *The biological meaning of Theorem 4 is that the population size in biological systems is often limited by the available resources. If the population size grows infinitely, the available resources will eventually be exhausted, resulting in the extinction of the population. Therefore, the boundedness of the solution can reflect the limitedness of resources and the sustainability of the population size. By considering the boundedness of the solution, the biomathematical model can more accurately describe the dynamic changes and interactions in the biological system, as well as the mechanisms to maintain biodiversity and ecological balance within a certain range.*

5. Stability of Equilibrium Points

In this section, we investigate the existence and stability of the equilibrium points of system (5). The equilibrium points are as follows:

(i) The trivial equilibrium point $E_0 = (0, 0, 0, 0)$ always exists.

(ii) The boundary equilibrium point $E_1 = (\tilde{x_1^s}, 0, \tilde{x_2}, 0)$ exists if and only if $\alpha\Omega > d_2\beta$ where

$$\tilde{x_1^s} = \frac{\alpha\tilde{x_2}}{\beta}, \quad \tilde{x_2} = \frac{\alpha\Omega - d_2\beta}{\beta\eta}.$$

(iii) If the following assumptions are satisfied:

Hypothesis 1. $\sigma > ad_3$.

Hypothesis 2. $\frac{\alpha\theta d_3}{\beta\varphi d_3 + \beta d_1 A} > 1$.

Hypothesis 3. $\frac{d_3(2d_1\Omega\varphi^2 + \psi\theta)A + \Omega\varphi^3 d_3^2}{(d_2\theta + d_1^2\Omega + d_1\beta\psi)A^2 + \theta\eta d_3 A + \Omega A^3} > 1$.

then the coexistence equilibrium point $E_2 = (x_1^{s*}, x_1^{i*}, x_2^*, y^*)$ exists, where

$$\begin{aligned}
&A = (1-m)(\sigma - ad_3), \quad x_1^i = \frac{\alpha x_2^* - \beta x_1^{s*}}{\theta x_1^{s*}},\\
&x_1^{s*} = \frac{\varphi x_2^* + d_1}{\theta}, \quad x_2^* = \frac{d_3}{(1-m)(\sigma - ad_3)},\\
&y^* = \frac{(\Omega x_1^s + \psi x_2^* x_1^{i*} - \eta x_2^{*2} - d_2 x_2^*)(1 + a(1-m))x_2^*}{\mu(1-m)x_2^*}.
\end{aligned}$$

Theorem 5. *The trivial equilibrium point E_0 is locally asymptotically stable if and only if $\beta d_2 > \alpha\Omega$.*

Proof. The Jacobian matrix for system (5) at E_0 is shown below

$$J(E_0) = \begin{pmatrix} -\beta & 0 & \alpha & 0 \\ 0 & -d_1 & 0 & 0 \\ \Omega & 0 & -d_2 & 0 \\ 0 & 0 & 0 & -d_3 \end{pmatrix}, \tag{18}$$

with characteristic equation

$$(\lambda + d_1)(\lambda + d_3)\{\lambda^2 + (\beta + d_2)\lambda + \beta d_2 - \alpha\Omega\} = 0. \tag{19}$$

The eigenvalues of (19) are

$$\lambda_1 = -d_1,\ \lambda_2 = -d_3,\ \lambda_{3,4} = \frac{-(\beta + d_2) \pm \sqrt{(\beta + d_2)^2 - 4(\beta d_2 - \alpha\Omega)}}{2}. \tag{20}$$

It is easy to see that

$$\mid arg(\lambda_{(1,2)}) \mid = \pi > \frac{\pi\varrho}{2}. \tag{21}$$

To find the principal values of parameters λ_3 and λ_4, we consider two cases.

Case a: $\beta d_2 < \alpha\Omega$ and then $(\beta + d_2)^2 - 4(\beta d_2 - \alpha\Omega) > 0$. By (20), this yields $\lambda_3 < 0$ and $\lambda_4 > 0$. Hence,

$$\mid \arg(\lambda_3) \mid = \pi > \frac{\pi\varrho}{2}, \quad \mid \arg(\lambda_4) \mid = 0 < \frac{\pi\varrho}{2}, \tag{22}$$

for all $0 < \varrho \leq 1$. Based on Theorem 2, the trivial equilibrium point E_0 is unstable.

Case b: If $\beta d_2 > \alpha\Omega$, there are two situations; they are

$$A(1): \quad (d_2+\beta)^2 - 4(\beta d_2 - \alpha\Omega) \geq 0,$$

or

$$A(2): \quad (d_2+\beta)^2 - 4(\beta d_2 - \alpha\Omega) < 0.$$

If A(1) holds, then $\lambda_3 < 0$ and $\lambda_4 < 0$. Hence,

$$|\arg(\lambda_{3,4})| = \frac{\pi}{2} > \frac{\pi\varrho}{2}. \tag{23}$$

If A(2) holds, then the eigenvalues of $J(E_0)$ are a pair of complex conjugates λ_3 and $\overline{\lambda_3}$, which yields

$$Re(\lambda_3) = Re(\overline{\lambda_3}). \tag{24}$$

By Equation (24), we can obtain

$$|\arg(\lambda_i)| > \frac{\pi}{2} > \frac{\pi\varrho}{2}. \tag{25}$$

Therefore, the equilibrium point E_0 is locally asymptotically stable if $\beta d_2 > \alpha\Omega$. This completes the proof. □

Theorem 6. *The boundary equilibrium point E_1 is unstable.*

Proof. The Jacobian matrix of system (5) at E_1 is provided as

$$J(E_1) = \begin{pmatrix} -\beta & -\theta\tilde{x}_1^s & \alpha & 0 \\ 0 & m_1 & 0 & 0 \\ \Omega & \psi\tilde{x}_2 & m_2 & m_3 \\ 0 & 0 & 0 & m_5 \end{pmatrix}, \tag{26}$$

where

$$m_1 = \theta\tilde{x}_1^s - \varphi\tilde{x}_2 - d_1, \quad m_2 = -2\eta\tilde{x}_2 - d_2,$$
$$m_3 = -\frac{\mu(1-m)\tilde{x}_2}{1+a(1+m)\tilde{x}_2}, \quad m_5 = \frac{\sigma(1-m)\tilde{x}_2}{1+a(1+m)\tilde{x}_2} - d_3.$$

The characteristic equation is

$$(\lambda - m_1)(\lambda - m_5)\{\lambda^2 + (\beta + m_2)\lambda + (m_2\beta - \alpha\Omega)\} = 0. \tag{27}$$

Because $m_2 < 0$, specifically $m_2\beta - \alpha\Omega < 0$, one eigenvalue of Equation (27) must possess a positive real component. By Theorem 2, E_1 is unstable. This completes the proof. □

Theorem 7. *The coexistence equilibrium point $E_2 = (x_1^{s*}, x_1^{i*}, x_2^*, y^*)$ of system (5) is locally asymptotically stable if Hypotheses 1–4 are established.*

Proof. The Jacobian matrix of system (5) at E_2 is

$$J(E_2) = \begin{pmatrix} h_{11} & h_{12} & \alpha & 0 \\ h_{21} & h_{22} & h_{23} & 0 \\ \Omega & h_{32} & h_{33} & h_{34} \\ 0 & 0 & h_{43} & h_{44} \end{pmatrix}, \tag{28}$$

where

$$h_{11} = -\beta - \theta x_1^{i*}, \quad h_{12} = -\theta x_1^{s*}, \quad h_{21} = \theta x_1^{i*}, \quad h_{22} = \theta x_1^{s*} - \varphi x_2^* - d_1,$$
$$h_{23} = -\varphi x_1^{i*}, h_{32} = \psi x_2^*, \quad h_{33} = \psi x_1^{i*} - \frac{\mu(1-m)y^*}{(1+a(1+m))^2} - 2\eta x_2^*,$$
$$h_{34} = -\frac{\mu(1-m)x_2^*}{1+a(1-m)x_2^*}, \quad h_{43} = \frac{\sigma(1-m)y^*}{(1+a(1+m))^2}, \quad h_{44} = \frac{\sigma(1-m)x_2^*}{1+a(1-m)x_2^*}.$$

So, the characteristic Equation (28) is as follows:

$$\lambda^4 + A_1\lambda^3 + A_2\lambda^2 + A_3\lambda + A_4 = 0, \tag{29}$$

where

$$\begin{aligned}
A_1 &= -(h_{11} + h_{22} + h_{33} + h_{44}),\\
A_2 &= h_{22}h_{44} + h_{33}h_{44} - h_{34}h_{43} + h_{11}h_{22} - h_{12}h_{21} + h_{11}h_{33} - \alpha\Omega + h_{22}h_{33} - h_{23}h_{32}\\
&\quad + h_{11}h_{44},\\
A_3 &= h_{12}h_{21}h_{44} - h_{11}h_{22}h_{44} - h_{11}h_{33}h_{44} + h_{11}h_{34}h_{43} + \alpha\Omega h_{44} - h_{22}h_{33}h_{44}\\
&\quad + h_{22}h_{34}h_{43} + h_{23}h_{32}h_{44} - h_{11}h_{22}h_{33} + h_{11}h_{23}h_{32} + h_{12}h_{21}h_{33} - h_{12}h_{23}\Omega\\
&\quad - \alpha h_{21}h_{32} + \alpha\Omega h_{22},\\
A_4 &= h_{11}h_{22}h_{33}h_{44} - h_{11}h_{22}h_{34}h_{43} - h_{11}h_{23}h_{32}h_{44} - h_{12}h_{21}h_{33}h_{44} + h_{12}h_{21}h_{34}h_{43}\\
&\quad + \Omega h_{12}h_{23}h_{44} + \alpha h_{21}h_{32}h_{44} - \alpha\Omega h_{22}h_{44}.
\end{aligned}$$

Consider the following hypothesis:

Hypothesis 4. $A_1 > 0, A_2 > 0, A_3 > 0, \Delta_2 > 0, \Delta_3 > 0, \Delta_4 > 0$

where

$$\Delta_2 = \begin{vmatrix} A_1 & 1 \\ A_3 & A_2 \end{vmatrix}, \quad \Delta_3 = \begin{vmatrix} A_1 & 1 & 0 \\ A_3 & A_2 & A_1 \\ 0 & A_4 & A_3 \end{vmatrix}, \quad \Delta_4 = A_4\Delta_3.$$

By utilizing Hypothesis 4 and the Routh–Hurwitz criterion, it is shown that the eigenvalues of (29) have negative real parts. Thus, E_2 is locally asymptotically stable when $\tau = 0$. This completes the proof. □

In the following section, we investigate the Hopf bifurcation of system (5) with a time delay.

6. Hopf Bifurcation

For convenience, use the transformation

$$u_1^s(t) = x_1^s(t) - x_1^{s*}, \quad u_1^i(t) = x_1^i(t) - x_1^{i*},$$

$$u_2(t) = x_2(t) - x_2^*, \quad v(t) = y(t) - y^*.$$

Then, system (5) turns into:

$$
\begin{aligned}
{}^cD^{\varrho}u_1^s(t) &= \alpha(u_2(t)+x_2^*) - \beta(u_1^s(t)+x_1^{s*}) - \theta(u_1(t)+x_1^{s*})(u_1^i(t)+x_1^{i*}),\\
{}^cD^{\varrho}u_1^i(t) &= \theta(u_1(t)+x_1^{s*})(u_1^i(t)+x_1^{i*}) - \varphi(u_1^i+x_1^{i*})(u_2(t)+x_2^*) - d_1(u_1^i(t)+x_1^{i*}),\\
{}^cD^{\varrho}u_2(t) &= \Omega(u_1^s(t)+x_1^{s*}) + \psi(u_1^i+x_1^{i*})(u_2(t)+x_2^*) - \eta(u_2(t)+x_2^*)^2\\
&\quad - \frac{a(u_2+x_2^*)(v+y^*)}{1+a(1-m)(u_2+x_2^*)} - d_2(u_2(t)+x_2^*),\\
{}^cD^{\varrho}v(t) &= \frac{b(u_2(t-\tau)+x_2^*)(v(t-\tau)+y^*)}{1+a(1-m)(u_2(t-\tau)+x_2^*)} - d_3(v(t)+y^*).
\end{aligned} \tag{30}
$$

From system (30), we can obtain

$$
\begin{aligned}
{}^cD^{\varrho}u_1^s(t) &= p_{11}u_1^s(t) + p_{12}u_1^i(t) + p_{13}x_2(t),\\
{}^cD^{\varrho}u_1^i(t) &= p_{21}u_1^s(t) + p_{22}u_1^i(t) + p_{23}u_2(t),\\
{}^cD^{\varrho}u_2(t) &= p_{31}u_1^s(t) + p_{32}u_1^i(t) + p_{33}u_2(t) + p_{34}v(t),\\
{}^cD^{\varrho}v(t) &= p_{44}v(t) + q_{43}u_2(t-\tau) + q_{44}v(t-\tau),
\end{aligned} \tag{31}
$$

where

$$
\begin{aligned}
&p_{11} = -\beta - \theta x_1^{i*}, \quad p_{12} = -\theta x_1^{s*}, \quad p_{13} = \alpha, \quad p_{21} = \theta x_1^{i*},\\
&p_{22} = \theta x_1^{s*} - \varphi x_2^* - d_1, \quad p_{23} = -\varphi x_1^{i*}, \qquad p_{34} = -\frac{a x_2^* y^*}{1+a(1-m)x_2^*},\\
&p_{31} = \Omega, \quad p_{32} = \psi x_2^*, \quad p_{33} = \psi x_1^{i*} - 2\eta x_2^* - d_2 - \frac{a y^*}{(1+a(1-m)x_2^*)^2},\\
&p_{44} = -d_3, \quad q_{43} = \frac{b y^*}{(1+a(1-m)x_2^*)^2}, \quad q_{44} = -\frac{b x_2^* y^*}{1+a(1-m)x_2^*}.
\end{aligned}
$$

Using the Laplace transform [20] on both sides of the equation of system (31) yields

$$
\begin{cases}
s^{\varrho}\pounds[u_1^s(t)] - s^{\varrho-1}\phi_1(0) = p_{11}\pounds[u_1^s(t)] - p_{12}\pounds\left[u_1^i(t)\right] - p_{13}\pounds[u_2(t)],\\
s^{\varrho}\pounds\left[u_1^i(t)\right] - s^{\varrho-1}\phi_2(0) = p_{21}\pounds[u_1^s(t)] + p_{22}\pounds\left[u_1^i(t)\right] + p_{23}\pounds[u_2(t)],\\
s^{\varrho}\pounds[u_2(t)] - s^{\varrho-1}\phi_3(0) = p_{31}\pounds[u_1^s(t)] + p_{32}\pounds\left[u_1^i(t)\right] + p_{33}\pounds[u_2(t)] + p_{34}\pounds[v(t)],\\
s^{\varrho}\pounds[v(t)] - s^{\varrho-1}\phi_4(0) = p_{44}\pounds[v(t)] + q_{43}e^{-s\tau}\left(\pounds[u_2(t)] + \int_{-\tau}^{0} e^{-st}\phi_3(t)dt\right)\\
\qquad\qquad + q_{44}e^{-s\tau}\left(\pounds[v(t)] + \int_{-\tau}^{0} e^{-st}\phi_4(t)dt\right),
\end{cases}
$$

which can be rewritten as:

$$
\Delta(\mathrm{s}) \cdot \begin{pmatrix} \pounds\left[u_1^s(t)\right] \\ \pounds\left[u_1^i(t)\right] \\ \pounds[u_2(t)] \\ \pounds[v(t)] \end{pmatrix} = \begin{pmatrix} \varsigma_1(s) \\ \varsigma_2(s) \\ \varsigma_3(s) \\ \varsigma_4(s) \end{pmatrix}, \tag{32}
$$

where

$$
\begin{aligned}
&\varsigma_1(s) = s^{\varrho-1}\phi_1(0), \quad \varsigma_2(s) = s^{\varrho-1}\phi_2(0), \quad \varsigma_3(s) = s^{\varrho-1}\phi_3(0),\\
&\varsigma_4(s) = s^{\varrho-1}\phi_4(0) + q_{43}e^{-s\tau}\textstyle\int_{-\tau}^{0} e^{-st}\phi_3(t)dt + q_{44}e^{-s\tau}\int_{-\tau}^{0} e^{-st}\phi_4(t)dt.
\end{aligned}
$$

The characteristic equation of Equation (32) is

$$\begin{vmatrix} s^{\varrho}-p_{11} & -p_{12} & -p_{13} & 0 \\ -p_{21} & s^{\varrho}-p_{22} & -p_{23} & 0 \\ -p_{31} & -p_{32} & s^{\varrho}-p_{33} & -p_{34} \\ 0 & 0 & -q_{43}e^{-s\tau} & s^{\varrho}-p_{44}-q_{44}e^{-s\tau} \end{vmatrix} = 0. \tag{33}$$

Equation (33) can be written as

$$\Gamma_1(s) + \Gamma_2(s)e^{-s\tau} = 0, \tag{34}$$

where

$$\begin{aligned}
\Gamma_1(s) =& s^{4\varrho} - (p_{11}+p_{22}+p_{33}+p_{44})s^{3\varrho} + (p_{22}p_{33} - p_{32}p_{34} + p_{44}p_{11} + p_{44}p_{22} \\
&+ p_{44}p_{33} + p_{11}p_{22} - p_{12}p_{21} - p_{13}p_{31} + p_{11}p_{33} - p_{23}p_{32} + p_{11}p_{23})s^{2\varrho} \\
&+ (p_{13}p_{22}p_{31} - p_{12}p_{23}p_{31} - p_{13}p_{21}p_{32} - p_{11}p_{22}p_{33} + p_{12}p_{21}p_{33} + p_{11}p_{32}p_{34} \\
&+ p_{22}p_{32}p_{34} - p_{11}p_{22}p_{44} + p_{12}p_{21}p_{44} + p_{13}p_{31}p_{44} - p_{11}p_{33}p_{44} + p_{23}p_{32}p_{44} \\
&- p_{22}p_{33}p_{44})s^{\varrho} + p_{12}p_{23}p_{31}p_{44} - p_{11}p_{23}p_{32}p_{44} + p_{13}p_{21}p_{32}p_{44} - p_{13}p_{22}p_{31}p_{44} \\
&+ p_{11}p_{22}p_{33}p_{44} - p_{12}p_{21}p_{33}p_{44} - p_{11}p_{22}p_{32}p_{34} + p_{12}p_{21}p_{32}p_{34}, \\
\Gamma_2(s) =& -s^{3\varrho}q_{44} + (p_{11}+p_{22}+p_{33})q_{44}s^{2\varrho} + (p_{12}p_{21} - p_{11}p_{22} + p_{13}p_{31} - p_{11}p_{33} \\
&+ p_{23}p_{32} - p_{22}p_{33})q_{44}s^{\varrho} + (p_{11}p_{23}p_{32} + p_{12}p_{23}p_{31} + p_{13}p_{21}p_{31} - p_{13}p_{22}p_{31} \\
&+ p_{11}p_{22}p_{33} - p_{12}p_{21}p_{33})q_{44}.
\end{aligned}$$

On the one hand, in order to find the critical value of the delay for which the stability of system (32) switches, one can assume

$$\mathrm{A}(3): \quad |\Gamma_1(0)| < |\Gamma_2(0)|. \tag{35}$$

Assume that $s = \kappa i = \kappa(\cos\frac{\pi}{2} + i\sin\frac{\pi}{2})(\kappa > 0)$ is a purely imaginary root of Equation (34); then, it follows that

$$\begin{cases} \hbar_1\cos\kappa\tau + \hbar_2\sin\kappa\tau = -\hbar_3, \\ \hbar_2\cos\kappa\tau - \hbar_1\sin\kappa\tau = -\hbar_4. \end{cases} \tag{36}$$

where

$$\begin{aligned} \hbar_1 &= \mathrm{Re}(\Gamma_2(i\kappa)), \quad \hbar_2 = \mathrm{Im}(\Gamma_2(i\kappa)), \\ \hbar_3 &= \mathrm{Re}(\Gamma_1(i\kappa)), \quad \hbar_4 = \mathrm{Im}(\Gamma_1(i\kappa)). \end{aligned}$$

The specific expression of $\hbar_i(i = 1, 2, 3, 4)$ is given in Appendix A.

Based on (36), the following results can be obtained:

$$\begin{cases} \sin\kappa\tau = \frac{\hbar_1\hbar_4 - \hbar_2\hbar_3}{\hbar_1^2+\hbar_2^2} = \chi_1(\kappa), \\ \cos\kappa\tau = -\frac{\hbar_3\hbar_1 + \hbar_2\hbar_4}{\hbar_1^2+\hbar_2^2} = \chi_2(\kappa). \end{cases} \tag{37}$$

It is apparent from (37) that

$$\chi_1(\kappa)^2 + \chi_2(\kappa)^2 = 1. \tag{38}$$

On the other hand, by (34), we can obtain

$$|\Gamma_1(\kappa i)| = |\Gamma_2(\kappa i)|. \tag{39}$$

As a matter of fact

$$\begin{aligned} |\Gamma_2(i\kappa)| - |\Gamma_1(i\kappa)| &\le |\Gamma_2(i\kappa)| - \left(\left|(i\kappa)^{3\varrho}\right| - \left|\Gamma_1(i\kappa) - (i\kappa)^{3\varrho}\right|\right) \\ &= -(i\kappa)^{3\varrho} + |\Gamma_2(i\kappa)| + \left|\Gamma_1(i\kappa) - (i\kappa)^{3\varrho}\right|. \end{aligned} \tag{40}$$

By limiting both sides of (40)

$$\lim_{\kappa \to +\infty} (|\Gamma_2(i\kappa)| - |\Gamma_1(i\kappa)|) = -\infty. \tag{41}$$

Because of assumption A(3), the equation $|\Gamma_1(i\kappa)| = |\Gamma_2(i\kappa)|$ has at least one positive solution. In addition, by combining Equation (36), the value of κ can be found. Finally, we find that the specific expression of time delay τ is

$$\tau^{(n)} = \frac{1}{\omega}[\arccos \boldsymbol{\Theta}_1(\kappa) + 2n\pi], \quad n = 0, 1, 2, \ldots \tag{42}$$

Due to (42), define the bifurcation point as

$$\tau_0 = \min\{\tau_n\}, n = 0, 1, 2, \ldots, \tag{43}$$

where τ_n is defined by (42).

In order to find the conditions under which Hopf bifurcation occurs, we give a necessary hypothesis:

Hypothesis 5. $\frac{\Theta_1\Xi_1+\Theta_2\Xi_2}{\Xi_1^2+\Xi_2^2} > 0$

where the expressions of Θ_i, Ξ_i $(i = 1, 2)$ are defined in (46).

From the above basic theoretical results, we present an important lemma in this section.

Lemma 1. *If hypothesis Hypothesis 5 holds, let $s(\tau) = \phi(\tau) + i\kappa(\tau)$ be the root of Equation (34) near $\tau = \tau_j$ satisfying $\phi(\tau_j) = 0, \kappa(\tau_j) = \kappa_0$. Then, the following transversality condition holds*

$$\mathrm{Re}\left[\frac{ds(\tau)}{d\tau}\right]\Big|_{(\tau=\tau_0,\kappa=\kappa_0)} > 0.$$

Proof. By differentiating both sides of (34) with regard to τ, one obtains

$$\Gamma_1'(s)\frac{ds}{d\tau} + \Gamma_2'(s)e^{-s\tau}\frac{ds}{d\tau} + \Gamma_2(s)e^{-s\tau}\left(-\tau\frac{ds}{d\tau} - s\right) = 0, \tag{44}$$

where $\Gamma_i'(s)$ is the derivative of $\Gamma_i(s)$ $(i = 1, 2)$. Based on (44), we claim that

$$\frac{ds}{d\tau} = \frac{\Theta(s)}{\Xi(s)}, \tag{45}$$

where

$$\begin{aligned}\Theta(s) = {} & -s^{3\varrho+1}q_{44}e^{-s\tau} + (p_{11} + p_{22} + p_{33})q_{44}s^{2\varrho+1}e^{-s\tau} + (p_{12}p_{21} - p_{11}p_{22} \\ & + p_{13}p_{31} - p_{11}p_{33} + p_{23}p_{32} - p_{22}p_{33})q_{44}s^{\varrho+1}e^{-s\tau} + se^{-s\tau}(p_{11}p_{23}p_{32} \\ & + p_{12}p_{23}p_{31} + p_{13}p_{21}p_{31} - p_{13}p_{22}p_{31} + p_{11}p_{22}p_{33} - p_{12}p_{21}p_{33})q_{44},\end{aligned}$$

$$\begin{aligned}\Xi(s) &= \Gamma_1'(s) + \Gamma_2'(s)e^{-s\tau} - \tau\Gamma_2(s)e^{-s\tau}\\ &= 4\varrho s^{4\varrho-1} - 3\varrho s^{3\varrho-1}(p_{11}+p_{22}+p_{33}+p_{44}) + 2\varrho s^{2\varrho-1}(p_{22}p_{33} - p_{32}p_{34} + p_{44}p_{11}\\ &\quad + p_{44}p_{22} + p_{44}p_{33} + p_{11}p_{22} - p_{12}p_{21} - p_{13}p_{31} + p_{11}p_{33} - p_{23}p_{32} + p_{11}p_{23})\\ &\quad + (p_{13}p_{22}p_{31} - p_{12}p_{23}p_{31} - p_{13}p_{21}p_{32} - p_{11}p_{22}p_{33} + p_{12}p_{21}p_{33} + p_{11}p_{32}p_{34}\\ &\quad + p_{22}p_{32}p_{34} - p_{11}p_{22}p_{44} + p_{12}p_{21}p_{44} + p_{13}p_{31}p_{44} - p_{11}p_{33}p_{44} + p_{23}p_{32}p_{44}\\ &\quad - p_{22}p_{33}p_{44})\varrho s^{\varrho-1} + e^{-s\tau}\{-3\varrho s^{3\varrho-1}q_{44} + (p_{11}+p_{22}+p_{33})q_{44}2\varrho s^{2\varrho-1}\\ &\quad + (p_{12}p_{21} - p_{11}p_{22} + p_{13}p_{31} - p_{11}p_{33} + p_{23}p_{32} - p_{22}p_{33})q_{44}\varrho s^{\varrho-1}\} - \tau e^{s\tau}\\ &\quad \{-s^{3\varrho}q_{44} + (p_{11}+p_{22}+p_{33})q_{44}s^{2\varrho} + (p_{12}p_{21} - p_{11}p_{22} + p_{13}p_{31} - p_{11}p_{33}\\ &\quad + p_{23}p_{32} - p_{22}p_{33})q_{44}s^{\varrho} + (p_{11}p_{23}p_{32} + p_{12}p_{23}p_{31} + p_{13}p_{21}p_{31} - p_{13}p_{22}p_{31}\\ &\quad + p_{11}p_{22}p_{33} - p_{12}p_{21}p_{33})q_{44}\}.\end{aligned}$$

It can be deduced from Equation (45) that

$$\mathrm{Re}\left[\frac{ds(\tau)}{d\tau}\right]\Big|_{(\tau=\tau_0,\kappa=\kappa_0)} = \frac{\Theta_1\Xi_1 + \Theta_2\Xi_2}{\Xi_1^2 + \Xi_2^2}, \tag{46}$$

where the expressions of Θ_i, Ξ_i $(i = 1, 2)$ are given in Appendix B.

From assumption Hypothesis 5, we have completed the proof of Lemma 1. □

Theorem 8. *For system (5), if Hypotheses 1–5 and A(3) hold, then one can obtain the following results.*

(i) If $\tau \in [0, \tau_0)$, then the coexistence equilibrium E_2 of system (5) is asymptotically stable.
(ii) The coexistence equilibrium E_2 of system (5) is unstable when $\tau > \tau_0$.
(iii) If $\tau = \tau_0$, then system (5) undergoes a Hopf bifurcation.

Remark 2. *This study investigates the bifurcation behavior and stability of a class of delayed fractional-order predation models with disease and cannibalism in the prey. In particular, comparing with existing models [20–27], we consider the stage structure, cannibalism, and diseases for the prey population. In addition, the dynamical interaction between the predator and the mature prey is described by the Holling type-II functional response function, and the influence of prey refuge is considered. Therefore, model (5) and the results obtained in this paper can be seen as a supplement to and extensions of previous studies [20–27].*

7. Numerical Simulations

Numerical simulations of fractional-delay differential system (5) were performed using the Adams–Bashforth–Moulton predictive correction method to validate the feasibility of the theoretical analysis in [43]. The detailed algorithm of the Adams–Bashforth–Moulton predictive correction method for system (5) is given in Appendix C. Consider the following parameter values:

$$\begin{aligned}&\alpha = 3, \quad \beta = 1.15, \quad \theta = 0.3, \quad \varphi = 0.15, \quad d_1 = 0.3, \quad \Omega = 1, \quad a = 0.1,\\ &\mu = 0.25, \quad m = 0.25, \quad \psi = 0.1, \quad \eta = 0.1, \quad d_2 = 0.15, \quad \sigma = 0.2, \quad d_3 = 0.18,\end{aligned}$$

and the initial values $(x_1^s(0), x_1^i(0), x_2(0), y(0)) = (2, 3, 2, 7)$. By direct calculation, we obtain

$$\sigma - ad_3 \approx 0.18, \frac{\alpha\theta d_3}{\beta\varphi d_3 + \beta d_1 A} \approx 2.07, \frac{d_3(2d_1\Omega\varphi^2 + \psi\theta)A + \Omega\varphi^3 d_3^2}{(d_2\theta + d_1^2\Omega + d_1\beta\psi)A^2 + \theta\eta d_3 A + \Omega A^3} \approx 1.0052.$$

Then, we know that conditions Hypotheses 1–5 are true, and the coexistence of equilibrium point $E_2 = (x_1^{s*}, x_1^{i*}, x_2^*, y^*) = (1.74, 1.48, 4.67, 11.41)$ is proven. We will now study the effects of some important parameters in the system on the system dynamics.

Case 1: The influence of fractional orders on the stability region.

We assume $\tau = 0$, and first discuss the effect of the fractional order on the rate of the equilibrium point of solution convergence. To ensure the reliability of the numerical simulation results, we initially disregarded the effect of the time delay on the system stability by setting $\tau = 0$.

Figures 1 and 2 show the local asymptotic stability of the equilibrium point of the system for various orders. In Figure 1a–d, for the orders $\varrho = 0.85, 0.9$, and 0.95, the oscillatory behavior of the solution intensifies as the order increases. A shift from stability to instability occurred in the system solution as the order rose from 0.95 to 0.99, as shown in Figure 2a–d. This transition highlights the significant effect of the order of a fractional-order system in the stable region.

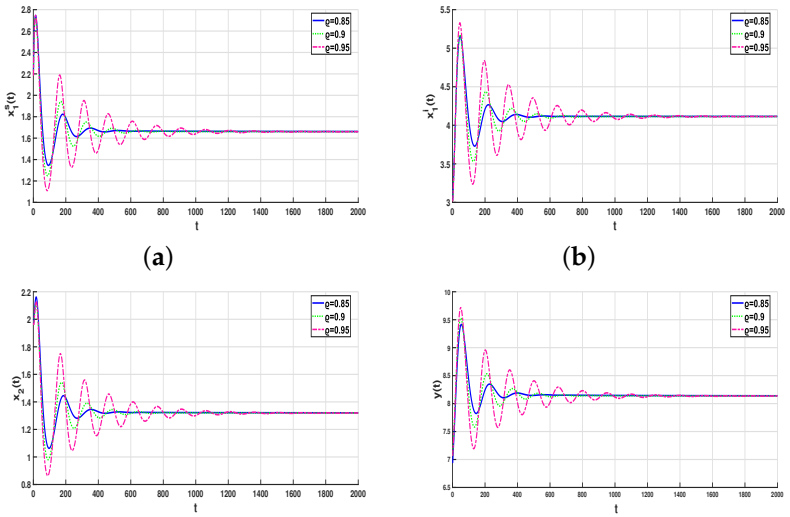

Figure 1. Local asymptotic stability diagram of system at E_2 when $\varrho = 0.85, 0.9, 0.95$. (**a**) Stability of $x_1^s(t)$ when $\varrho = 0.85, 0.9, 0.95$. (**b**) Stability of $x_1^i(t)$ when $\varrho = 0.85, 0.9, 0.95$. (**c**) Stability of $x_2(t)$ when $\varrho = 0.85, 0.9, 0.95$. (**d**) Stability of $y(t)$ when $\varrho = 0.85, 0.9, 0.95$.

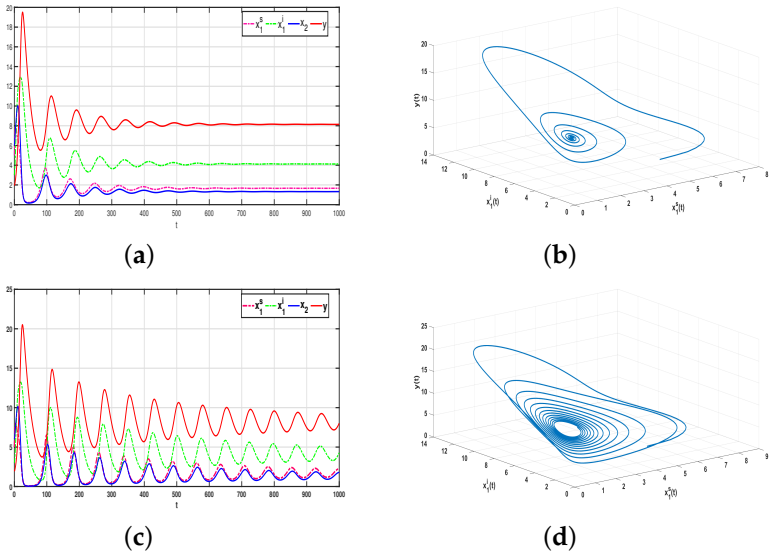

Figure 2. Dynamical behavior of system (5) under different ϱ. (**a**,**b**) are the time series and phase diagram when $\varrho = 0.95$; (**c**,**d**) are the time series diagram and phase diagram when $\varrho = 0.99$.

Remark 3. *When $\varrho = 1$, the fractional-order system transforms into an integer-order system, and at this time, the integer-order system should be unstable because the fractional-order system has already*

shown an unstable state when $\varrho = 0.99$. Therefore, the stability domain of the fractional-order system is much larger than that of the integer-order system. The biological explanation is as follows: the population will use past experience to produce an impact on the current behavior, thus explaining the memory effect in animal behavior. Such memory is more beneficial to the long-term development of the species.

Case 2: The effect of cannibalism on disease.

By keeping the above parameters unchanged with a time delay of $\tau = 0$, we examined the effects of altering the values of φ and ψ on the number of infected prey in the young prey category. Specifically, we tested φ values of 0.15, 0.35, and 0.65, combined with ψ values of 0.1, 0.25, and 0.45. The results of these variations are depicted in Figure 3a–f, where (a) and (d), (b) and (e), and (c) and (f) represent the waveform and phase diagrams of system (5) in the vicinity of E_2 for $\varphi = 0.15$ and $\psi = 0.1$, for $\varphi = 0.35$ and $\psi = 0.2$, and for $\varphi = 0.65$ and $\psi = 0.4$, respectively. As φ increases, signifying a higher predation of infection by adult prey in the population, the number of infected populations exhibits a decreasing trend, ultimately leading to potential extinction. This suggests that cannibalism plays a crucial role in restraining disease propagation.

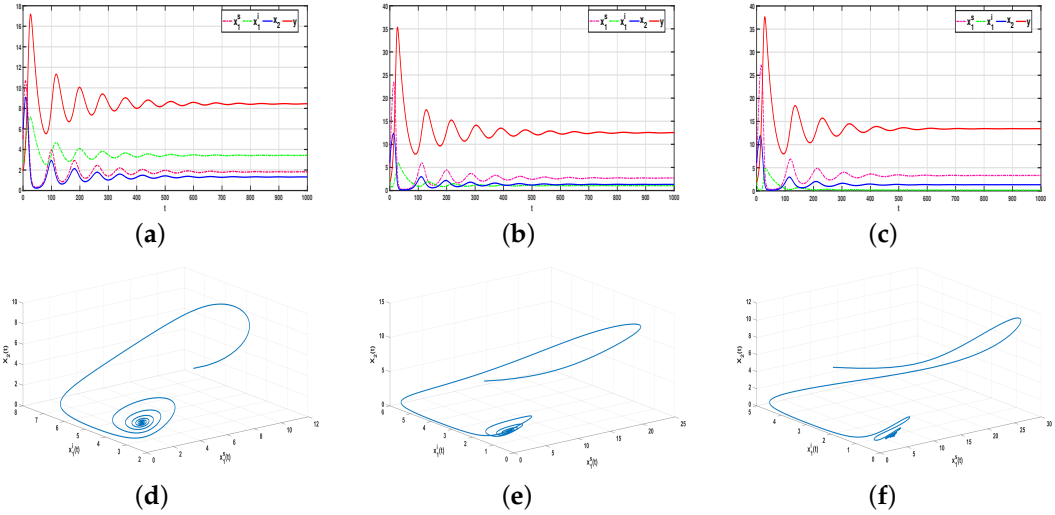

Figure 3. Waveform plot and phase portrait of the system (5) near E_3 when $\varrho = 0.95$. Where (**a**) and (**d**) represent the waveform and phase diagrams of system (5) in the vicinity of E_2 for $\varphi = 0.15$ and $\psi = 0.1$; (**b**,**e**) represent the waveform and phase diagrams of system (5) in the vicinity of E_2 for $\varphi = 0.35$ and $\psi = 0.2$; (**c**,**f**) represent the waveform and phase diagrams of system (5) in the vicinity of E_2 for $\varphi = 0.65$ and $\psi = 0.4$.

Remark 4. *The adult prey killing the sick juvenile individuals plays a role in controlling the spread of diseases. Through cannibalism, the juvenile individuals infected with the pathogen are predated and digested, and this behavior helps to eliminate or reduce the transmission rate of the pathogen from the juvenile group, which can reduce potential disease outbreaks in the group and help to maintain the overall health of the group. In addition, by eliminating sick and vulnerable individuals, cannibalism can promote the survival and reproduction of the genetically superior individuals.*

Case 3: The effect of time delays on system stability and Hopf bifurcation

In this section, we take a time delay as the bifurcation parameter to explore the stability of the time delay at the equilibrium point E_2 and the Hopf bifurcation phenomenon. A numerical analysis was conducted to demonstrate the influence of a delay in system (5) with $\varrho = 0.9$. Thus, according to Theorem 8, system (5) experiences a Hopf bifurcation at the equilibrium point E_2 when $\tau_0 = 0.95$. To be specific, system (5) is locally asymptotically stable at the equilibrium point E_2 when $\tau = 0.88 < \tau_0$, as shown in Figure 4a–c. Conversely, when $\tau = 1.3 > \tau_0$, the system transitions from a stable to an unstable state, leading to the

emergence of a family of oscillations, as shown in Figure 5a–c. Consequently, surpassing the critical value τ_0 indicates that system (5) exhibits Hopf bifurcation originating from the coexistence equilibrium E_2.

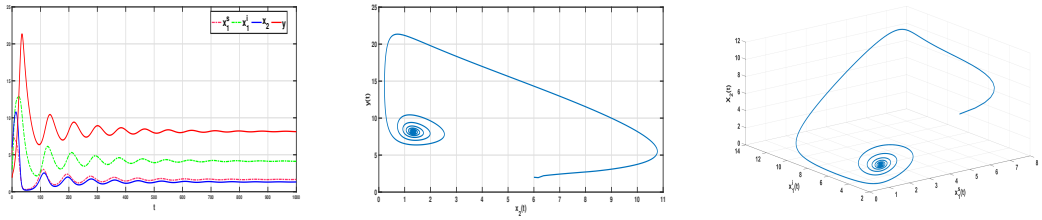

(**a**) (**b**) (**c**)

Figure 4. Waveform plots and phase portraits of system (5) when $\varrho = 0.9, \tau = 0.88 < \tau_0 = 0.95$. (**a**) Stability of $x_1^s(t)$, $x_1^i(t)$, $x_2(t)$ and $y(t)$ when $\varrho = 0.9, \tau = 0.88 < \tau_0 = 0.95$. (**b**) Stability of $x_2(t)$ and $y(t)$ when $\varrho = 0.9, \tau = 0.88 < \tau_0 = 0.95$. (**c**) Stability of $x_1^s(t)$, $x_1^i(t)$ and $x_2(t)$ when $\varrho = 0.9, \tau = 0.88 < \tau_0 = 0.95$.

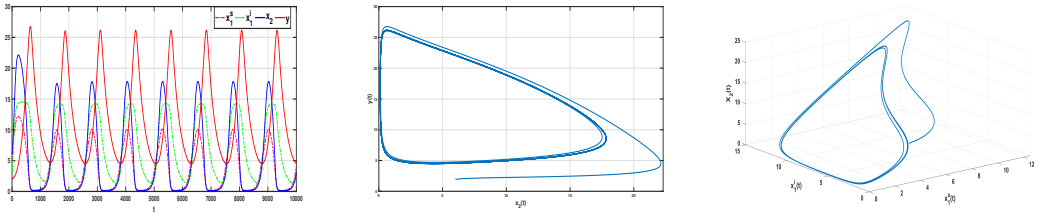

(**a**) (**b**) (**c**)

Figure 5. Dynamical behavior of system (5) when $\varrho = 0.9, \tau = 1.3 > \tau_0 = 0.95$. (**a**) Instability of $x_1^s(t)$, $x_1^i(t)$, $x_2(t)$ and $y(t)$ when $\varrho = 0.9, \tau = 1.3 > \tau_0 = 0.95$. (**b**) Instability of $x_2(t)$ and $y(t)$ when $\varrho = 0.9, \tau = 1.3 > \tau_0 = 0.95$. (**c**) Instability of $x_1^s(t)$, $x_1^i(t)$ and $x_2(t)$ when $\varrho = 0.9, \tau = 1.3 > \tau_0 = 0.95$.

To better demonstrate the effect of the fractional order, the value of ϱ was continuously adjusted in the subsequent simulation, with ϱ set at 0.95. Following the computation of the bifurcation point $\tau_0 = 0.35$, it becomes apparent that compared to the case of $\varrho = 0.9$, the original bifurcation point of 0.95 is reduced to 0.35. This reduction implies an increase in the bifurcation threshold. To enhance the comparative analysis, τ is set to 0.88, which is greater than $\tau_0 = 0.35$. From Figure 6a–c, it is evident that the solution is oscillatory, signaling a transition from the initial stable waveform and phase diagrams depicted in Figure 4 to an unstable state under the condition $\varrho = 0.95$.

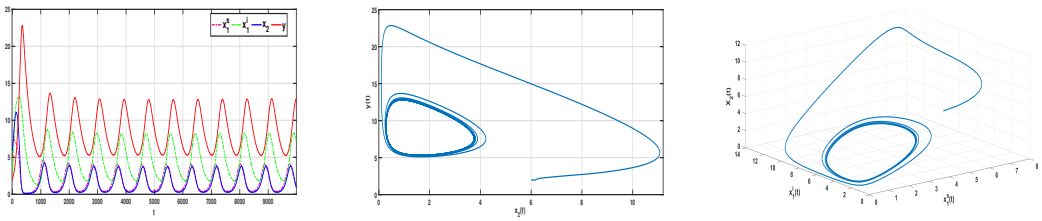

(**a**) (**b**) (**c**)

Figure 6. Dynamical behavior of system (5) when $\varrho = 0.95, \tau = 0.88 > \tau_0 = 0.35$. (**a**) Instability of $x_1^s(t)$, $x_1^i(t)$, $x_2(t)$ and $y(t)$ when $\varrho = 0.95, \tau = 0.88 > \tau_0 = 0.35$. (**b**) Instability of $x_2(t)$ and $y(t)$ when $\varrho = 0.95, \tau = 0.88 > \tau_0 = 0.35$. (**c**) Instability of $x_1^s(t)$, $x_1^i(t)$ and $x_2(t)$ when $\varrho = 0.95$, $\tau = 0.88 > \tau_0 = 0.35$.

By setting $\varrho = 0.85$ and calculating the fork point as $\tau_0 = 1.75$, a comparison can be made with the case when $\varrho = 0.95$. In the scenario where $\varrho = 0.95$, the bifurcation point is delayed from the initial value of 0.35 to 1.75, signifying a delay in the bifurcation threshold.

To establish a more comprehensive comparison, we consider $\tau = 0.88 < \tau_0 = 1.75$. By examining Figure 7a–c, we find that the solution of the system stabilizes, in contrast to the outcome shown in Figure 6. This observation enables us to understand the effect of the fractional-order sequence on the bifurcation point of the system. As illustrated in Figure 8, the bifurcation point steadily decreased as the fractional order increased. Conversely, a reduction in fractional order leads to a continuous backward delay at the bifurcation point.

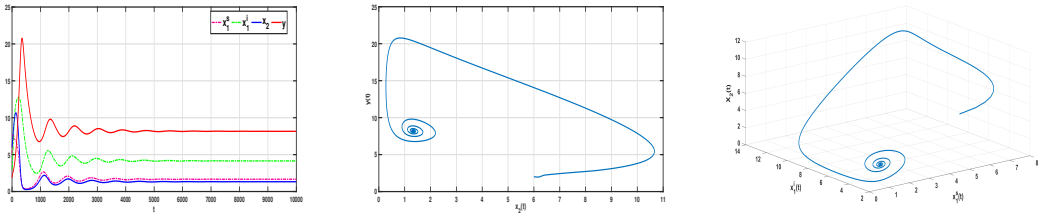

(**a**) (**b**) (**c**)

Figure 7. Dynamical behavior of system (5) when $\varrho = 0.85, \tau = 0.88 < \tau_0 = 1.75$. (**a**) Stability of $x_1^s(t)$, $x_1^i(t)$, $x_2(t)$ and $y(t)$ when $\varrho = 0.85, \tau = 0.88 < \tau_0 = 1.75$. (**b**) Stability of $x_2(t)$ and $y(t)$ when $\varrho = 0.85, \tau = 0.88 < \tau_0 = 1.75$. (**c**) Stability of $x_1^s(t)$, $x_1^i(t)$ and $x_2(t)$ when $\varrho = 0.85, \tau = 0.88 < \tau_0 = 1.75$.

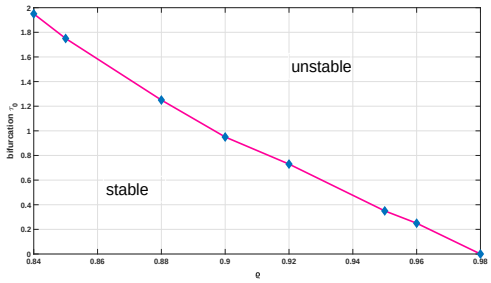

Figure 8. The effect of fractional-order sequence ϱ on bifurcation point τ_0.

Case 4: The effect of prey refuge on the system's stability and bifurcation

In this part, by keeping the other parameters unchanged with $\tau = 0$, for different values of m, we investigate the impact of prey refuge on the system. Hence, we set $m = 0.01, 0.4, 0.99$; the corresponding numerical simulation results of these variations are depicted in Figure 9. From the numerical simulation figures in Figure 9a–c and the values of m, we can see that as the value of m increases, the time for the system to reach stability exhibits a decreasing trend. Thus, appropriately increasing the value of m will contribute to the system reaching a stable state within a short period of time. However, if the value of m reaches 0.99, then it will directly lead to the extinction of the predator population, which is extremely detrimental to the development of the predator population.

Next, we explore the impact of the change in the value of m on system bifurcation. In Figure 6, we have calculated that when $m = 0.25$ and $\varrho = 0.95$, the system's Hopf bifurcation point is 0.35. In order to achieve a better comparison effect, here, we only change the value of m, and the other parameters are consistent with the parameters used in Figure 6. After setting $m = 0.4$, this time, the bifurcation point of the system becomes 0.55, as shown in Figure 10a–c and Figure 11a–c. After a comparison with Figure 6, it can be found that appropriately increasing the value of m will delay the time for system (5) to undergo Hopf bifurcation.

Remark 5. *The stability of the ecosystem requires maintaining the relative balance between each population. The prey population is moderately regulated by the predators, which helps to maintain the stability and function of the entire ecosystem. Reasonable protection measures should comprehensively consider the interaction between the prey and the predator to ensure the balance and stability of biodiversity and the ecosystem.*

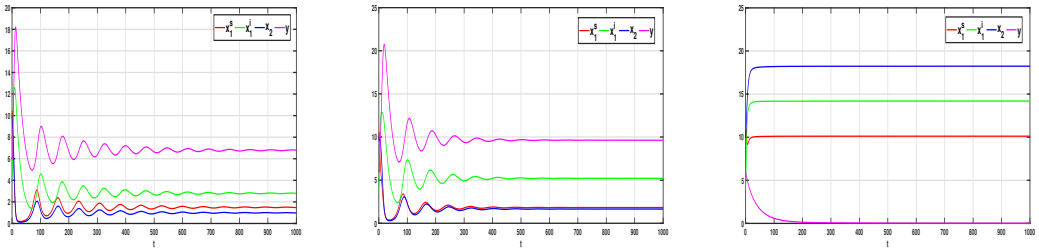

(**a**) (**b**) (**c**)

Figure 9. Dynamical behavior of system (5) when m = 0.01, 0.4, 0.99, where $\varrho = 0.95$. (**a**) Waveform plots of $x_1^s(t)$, $x_1^i(t)$, $x_2(t)$ and $y(t)$ when m = 0.01 and $\varrho = 0.95$. (**b**) Waveform plots of $x_1^s(t)$, $x_1^i(t)$, $x_2(t)$ and $y(t)$ when m = 0.4 and $\varrho = 0.95$. (**c**) Waveform plots of $x_1^s(t)$, $x_1^i(t)$, $x_2(t)$ and $y(t)$ when m = 0.99 and $\varrho = 0.95$.

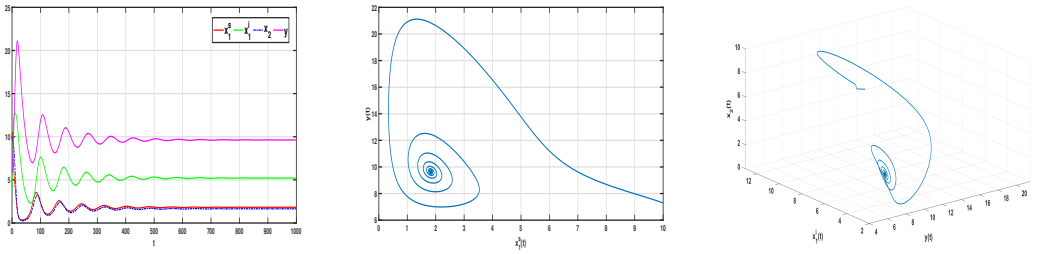

(**a**) (**b**) (**c**)

Figure 10. Dynamical behavior of system (5) when $\varrho = 0.95, \tau = 0.35 < \tau_0 = 0.55$, where m = 0.4. (**a**) Stability of $x_1^s(t)$, $x_1^i(t)$, $x_2(t)$ and $y(t)$ when $\varrho = 0.95, \tau = 0.35 < \tau_0 = 0.55$, where m = 0.4. (**b**) Stability of $x_1^s(t)$ and $y(t)$ when $\varrho = 0.95, \tau = 0.35 < \tau_0 = 0.55$,where m = 0.4. (**c**) Stability of $x_2(t)$, $x_1^i(t)$, and $y(t)$ when $\varrho = 0.95, \tau = 0.35 < \tau_0 = 0.55$, where m = 0.4.

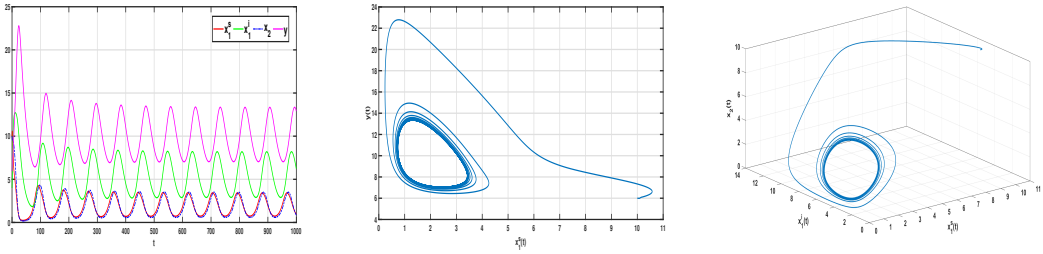

(**a**) (**b**) (**c**)

Figure 11. Dynamical behavior of system (5) when $\varrho = 0.95, \tau = 0.8 > \tau_0 = 0.55$, where m = 0.4. (**a**) Instability of $x_1^s(t)$, $x_1^i(t)$, $x_2(t)$ and $y(t)$ when $\varrho = 0.95, \tau = 0.8 > \tau_0 = 0.55$, where m = 0.4. (**b**) Instability of $x_1^s(t)$ and $y(t)$ when $\varrho = 0.95, \tau = 0.8 > \tau_0 = 0.55$, where m = 0.4. (**c**) Instability of $x_2(t)$, $x_1^i(t)$, and $y(t)$ when $\varrho = 0.95, \tau = 0.8 > \tau_0 = 0.55$, where m = 0.4.

8. Conclusions

In this study, stability and bifurcation problems of a class of delayed fractional-order PP systems with cannibalism and disease in the prey were studied. Disease, cannibalism, and the stage structure were examined in prey populations for the first time. We hypothesized that sick, immature prey might not develop into mature prey effectively. In prey populations afflicted with disease, mature individuals may choose to eat the sick offspring. This behavior exists in the animal kingdom and some species are known for cannibalism. In this system, predators primarily consume mature prey, and PP interactions are described using the Holling type-II functional response. Furthermore, we considered the protective role of prey refuge and developed a delayed fractional predator–prey model.

The existence of solutions, uniform boundedness, local stability, and Hopf bifurcations in the system was investigated. Numerical simulations demonstrated that in this unique

predation system, prey cannibalism contributes to disease extinction. In the numerical examples, it can be observed that diseased, immature prey gradually become extinct as predation by mature prey increases. Second, the fractional order has a significant effect on the stability of the entire system, and an increase in the fractional order can destroy the stability of the system. Compared with integer-order systems, fractional-order systems have more complex dynamics.

In addition, we found that a time delay can cause instability in the predation system, and the order can delay or advance the occurrence of Hopf bifurcation. Moreover, prey refuges have a significant impact on the stability of the considered system. Increasing the number of prey refuges can make the system reach the stable state earlier, and it can also delay the time of Hopf bifurcation. Future research will focus on the bifurcation of fractional-order time-delay systems and implementation controllers to mitigate bifurcation.

Author Contributions: Conceptualization, H.Z. and A.M.; methodology, H.Z.; software, H.Z.; validation, H.Z. and A.M.; formal analysis, H.Z. and A.M.; writing—original draft preparation, H.Z. and A.M.; writing—review and editing, H.Z. and A.M.; supervision, A.M. All authors have read and agreed to the published version of the manuscript.

Funding: This research was supported by the Open Project of Xinjiang Key Laboratory of Applied Mathematics (grant no. 2023D04045) and the National Natural Science Foundation of Xinjiang (grant no. 2021D01C067).

Data Availability Statement: No data were used to support this study.

Conflicts of Interest: The authors declare no conflicts of interest.

Appendix A

$$
\begin{aligned}
\hbar_1 =& -\kappa^{3\varrho}\cos\frac{3\varrho\pi}{2}q_{44}+\kappa^{2\varrho}\cos\frac{\varrho\pi}{2}(p_{11}+p_{22}+p_{33})q_{44}+\kappa^{\varrho}\cos\frac{\varrho\pi}{2}(p_{12}p_{21}-p_{11}p_{22}\\
&+p_{13}p_{31}-p_{11}p_{33}+p_{23}p_{32}-p_{22}p_{33})q_{44}+(p_{11}p_{23}p_{32}+p_{12}p_{23}p_{31}+p_{13}p_{21}p_{31}\\
&-p_{13}p_{22}p_{31}+p_{11}p_{22}p_{33}-p_{12}p_{21}p_{33})q_{44},\\
\hbar_2 =& -\kappa^{3\varrho}\sin\frac{3\varrho\pi}{2}q_{44}+\kappa^{2\varrho}\sin\frac{\varrho\pi}{2}(p_{11}+p_{22}+p_{33})q_{44}+\kappa^{\varrho}\sin\frac{\varrho\pi}{2}(p_{12}p_{21}-p_{11}p_{22}\\
&+p_{13}p_{31}-p_{11}p_{33}+p_{23}p_{32}-p_{22}p_{33})q_{44},\\
\hbar_3 =& \kappa^{4\varrho}\cos 2\varrho\pi-\kappa^{3\varrho}\cos\frac{3\rho\pi}{2}(p_{11}+p_{22}+p_{33}+p_{44})+\kappa^{2\varrho}\cos\varrho\pi(p_{22}p_{33}-p_{32}p_{34}\\
&+p_{44}p_{11}+p_{44}p_{22}+p_{44}p_{33}+p_{11}p_{22}-p_{12}p_{21}-p_{13}p_{31}+p_{11}p_{33}-p_{23}p_{32}+p_{11}p_{23})\\
&+\kappa^{\varrho}\cos\frac{\varrho\pi}{2}(p_{13}p_{22}p_{31}-p_{12}p_{23}p_{31}-p_{13}p_{21}p_{32}-p_{11}p_{22}p_{33}+p_{12}p_{21}p_{33}+p_{11}p_{32}p_{34}\\
&+p_{22}p_{32}p_{34}-p_{11}p_{22}p_{44}+p_{12}p_{21}p_{44}+p_{13}p_{31}p_{44}-p_{11}p_{33}p_{44}+p_{23}p_{32}p_{44}-p_{22}p_{33}p_{44})\\
&+p_{12}p_{23}p_{31}p_{44}-p_{11}p_{23}p_{32}p_{44}+p_{13}p_{21}p_{32}p_{44}-p_{13}p_{22}p_{31}p_{44}+p_{11}p_{22}p_{33}p_{44}\\
&-p_{12}p_{21}p_{33}p_{44}-p_{11}p_{22}p_{32}p_{34}+p_{12}p_{21}p_{32}p_{34},\\
\hbar_4 =& \kappa^{4\varrho}\sin 2\varrho\pi-\kappa^{3\varrho}\sin\frac{3\rho\pi}{2}(p_{11}+p_{22}+p_{33}+p_{44})+\kappa^{2\varrho}\sin\varrho\pi(p_{22}p_{33}-p_{32}p_{34}\\
&+p_{44}p_{11}+p_{44}p_{22}+p_{44}p_{33}+p_{11}p_{22}-p_{12}p_{21}-p_{13}p_{31}+p_{11}p_{33}-p_{23}p_{32}+p_{11}p_{23})\\
&+\kappa^{\varrho}\sin\frac{\varrho\pi}{2}(p_{13}p_{22}p_{31}-p_{12}p_{23}p_{31}-p_{13}p_{21}p_{32}-p_{11}p_{22}p_{33}+p_{12}p_{21}p_{33}+p_{11}p_{32}p_{34}\\
&+p_{22}p_{32}p_{34}-p_{11}p_{22}p_{44}+p_{12}p_{21}p_{44}+p_{13}p_{31}p_{44}-p_{11}p_{33}p_{44}+p_{23}p_{32}p_{44}-p_{22}p_{33}p_{44}).
\end{aligned}
$$

Appendix B

$$\begin{aligned}
\Theta_1 =& -\kappa_0^{3\varrho+1} q_{44}\cos(\frac{(3\varrho+1)\pi}{2}-\kappa_0\tau_0)+(p_{11}+p_{22}+p_{33})q_{44}\kappa_0^{2\varrho+1}\cos(\frac{(2\varrho+1)\pi}{2}-\kappa_0\tau_0)\\
&+(p_{12}p_{21}-p_{11}p_{22}+p_{13}p_{31}-p_{11}p_{33}+p_{23}p_{32}-p_{22}p_{33})q_{44}\kappa_0^{\varrho+1}\cos(\frac{(\varrho+1)\pi}{2}-\kappa_0\tau_0)\\
&+\kappa_0\cos(\frac{\pi}{2}-\kappa_0\tau_0)(p_{11}p_{23}p_{32}+p_{12}p_{23}p_{31}+p_{13}p_{21}p_{31}-p_{13}p_{22}p_{31}+p_{11}p_{22}p_{33}\\
&-p_{12}p_{21}p_{33})q_{44},\\
\Xi_1 =& 4\varrho\kappa_0^{4\varrho-1}\cos\frac{(4\varrho-1)\pi}{2}-3\varrho\kappa_0^{3\varrho-1}\cos\frac{(3\varrho-1)\pi}{2}(p_{11}+p_{22}+p_{33}+p_{44})\\
&+2\varrho\kappa_0^{2\varrho-1}\cos\frac{(2\varrho-1)\pi}{2}(p_{22}p_{33}-p_{32}p_{34}+p_{44}p_{11}+p_{44}p_{22}+p_{44}p_{33}+p_{11}p_{22}\\
&-p_{12}p_{21}-p_{13}p_{31}+p_{11}p_{33}-p_{23}p_{32}+p_{11}p_{23})+(p_{13}p_{22}p_{31}-p_{12}p_{23}p_{31}-p_{13}p_{21}p_{32}\\
&-p_{11}p_{22}p_{33}+p_{12}p_{21}p_{33}+p_{11}p_{32}p_{34}+p_{22}p_{32}p_{34}-p_{11}p_{22}p_{44}+p_{12}p_{21}p_{44}+p_{13}p_{31}p_{44}\\
&-p_{11}p_{33}p_{44}+p_{23}p_{32}p_{44}-p_{22}p_{33}p_{44})\varrho\kappa_0^{\varrho-1}\cos\frac{(\varrho-1)\pi}{2}-3\varrho\kappa_0^{3\varrho-1}q_{44}\cos(\frac{(3\varrho-1)\pi}{2}\\
&-\kappa_0\tau_0)+(p_{11}+p_{22}+p_{33})q_{44}2\varrho\kappa_0^{2\varrho-1}\cos(\frac{(2\varrho-1)\pi}{2}-\kappa_0\tau_0)+(p_{12}p_{21}-p_{11}p_{22}\\
&+p_{13}p_{31}-p_{11}p_{33}+p_{23}p_{32}-p_{22}p_{33})q_{44}\varrho\kappa_0^{\varrho-1}\cos(\frac{(\varrho-1)\pi}{2}-\kappa_0\tau_0)+\tau_0 q_{44}\kappa_0^{3\varrho}\cos\\
&(\frac{(3\varrho-1)\pi}{2}-\kappa_0\tau_0)-\tau_0(p_{11}+p_{22}+p_{33})q_{44}\kappa_0^{2\varrho}\cos(\varrho\pi-\kappa_0\tau_0)-\tau_0(p_{12}p_{21}-p_{11}p_{22}\\
&+p_{13}p_{31}-p_{11}p_{33}+p_{23}p_{32}-p_{22}p_{33})q_{44}\kappa_0^{\varrho}\cos(\frac{\varrho\pi}{2}-\kappa_0\tau_0)-\tau_0 q_{44}(p_{11}p_{23}p_{32}\\
&+p_{12}p_{23}p_{31}+p_{13}p_{21}p_{31}-p_{13}p_{22}p_{31}+p_{11}p_{22}p_{33}-p_{12}p_{21}p_{33})\cos(\kappa_0\tau_0),\\
\Theta_2 =& -\kappa_0^{3\varrho+1} q_{44}\sin(\frac{(3\varrho+1)\pi}{2}-\kappa_0\tau_0)+(p_{11}+p_{22}+p_{33})q_{44}\kappa_0^{2\varrho+1}\sin(\frac{(2\varrho+1)\pi}{2}-\kappa_0\tau_0)\\
&+(p_{12}p_{21}-p_{11}p_{22}+p_{13}p_{31}-p_{11}p_{33}+p_{23}p_{32}-p_{22}p_{33})q_{44}\kappa_0^{\varrho+1}\sin(\frac{(\varrho+1)\pi}{2}-\kappa_0\tau_0)\\
&+\kappa_0\cos(\frac{\pi}{2}-\kappa_0\tau_0)(p_{11}p_{23}p_{32}+p_{12}p_{23}p_{31}+p_{13}p_{21}p_{31}-p_{13}p_{22}p_{31}+p_{11}p_{22}p_{33}\\
&-p_{12}p_{21}p_{33})q_{44},\\
\Xi_2 =& 4\varrho\kappa_0^{4\varrho-1}\sin\frac{(4\varrho-1)\pi}{2}-3\varrho\kappa_0^{3\varrho-1}\sin\frac{(3\varrho-1)\pi}{2}(p_{11}+p_{22}+p_{33}+p_{44})\\
&+2\varrho\kappa_0^{2\varrho-1}\sin\frac{(2\varrho-1)\pi}{2}(p_{22}p_{33}-p_{32}p_{34}+p_{44}p_{11}+p_{44}p_{22}+p_{44}p_{33}+p_{11}p_{22}\\
&-p_{12}p_{21}-p_{13}p_{31}+p_{11}p_{33}-p_{23}p_{32}+p_{11}p_{23})+(p_{13}p_{22}p_{31}-p_{12}p_{23}p_{31}-p_{13}p_{21}p_{32}\\
&-p_{11}p_{22}p_{33}+p_{12}p_{21}p_{33}+p_{11}p_{32}p_{34}+p_{22}p_{32}p_{34}-p_{11}p_{22}p_{44}+p_{12}p_{21}p_{44}+p_{13}p_{31}p_{44}\\
&-p_{11}p_{33}p_{44}+p_{23}p_{32}p_{44}-p_{22}p_{33}p_{44})\varrho\kappa_0^{\varrho-1}\sin\frac{(\varrho-1)\pi}{2}-3\varrho\kappa_0^{3\varrho-1}q_{44}\sin(\frac{(3\varrho-1)\pi}{2}\\
&-\kappa_0\tau_0)+(p_{11}+p_{22}+p_{33})q_{44}2\varrho\kappa_0^{2\varrho-1}\sin(\frac{(2\varrho-1)\pi}{2}-\kappa_0\tau_0)+(p_{12}p_{21}-p_{11}p_{22}\\
&+p_{13}p_{31}-p_{11}p_{33}+p_{23}p_{32}-p_{22}p_{33})q_{44}\varrho\kappa_0^{\varrho-1}\sin(\frac{(\varrho-1)\pi}{2}-\kappa_0\tau_0)+\tau_0 q_{44}\kappa_0^{3\varrho}\sin\\
&(\frac{(3\varrho-1)\pi}{2}-\kappa_0\tau_0)-\tau_0(p_{11}+p_{22}+p_{33})q_{44}\kappa_0^{2\varrho}\sin(\varrho\pi-\kappa_0\tau_0)-\tau_0(p_{12}p_{21}-p_{11}p_{22}\\
&+p_{13}p_{31}-p_{11}p_{33}+p_{23}p_{32}-p_{22}p_{33})q_{44}\kappa_0^{\varrho}\sin(\frac{\varrho\pi}{2}-\kappa_0\tau_0)-\tau_0 q_{44}(p_{11}p_{23}p_{32}\\
&+p_{12}p_{23}p_{31}+p_{13}p_{21}p_{31}-p_{13}p_{22}p_{31}+p_{11}p_{22}p_{33}-p_{12}p_{21}p_{33})\sin(\kappa_0\tau_0).
\end{aligned}$$

Appendix C

Let the fractional-order system with delay be as follows

$$\begin{cases} {}^cD^{\varrho}H_j(t)=f_j(t,H_j(t),H_j(t-\tau)),t\in[-\tau,0],H_j^r(0)=H_{j0}^r,\\ r=0,1,2,\ldots,\lceil\varrho\rceil,j\in N, \end{cases}$$

where $L^r_{j0} \in R, \varrho > 0$ and

$$H_j(t) = \sum_{n=0}^{\lceil \varrho \rceil - 1} H^r_{j0} \frac{t^n}{n!} + \frac{1}{\Gamma(\varrho)} \int_0^t (t-s)^{\varrho-1} f_j(s, H_j(s), H_j(s-\tau)) ds, j \in N.$$

Let $h = \frac{T}{i}, t_n = nh, n = 0, 1, 2, \ldots, i$. Then, the corrector formulae are as follows:

$$\begin{aligned}
x^s_{1n+1} =& x^s_1(0) + \frac{h^\varrho}{\Gamma(\varrho+2)}(\alpha {x_2}^p_{n+1} - \beta {x^s_1}^p_{n+1} - \theta {x^s_1}^p_{n+1} {x^i_1}^p_{n+1}) + \frac{h^\varrho}{\Gamma(\varrho+2)} \sum_{j=0}^{n} \varpi_{j,n+1}(\alpha x_{2j} \\
& - \beta x^s_{1j} - \theta x^s_{1j} x^i_{1j}), \\
x^i_{1n+1} =& x^i_1(0) + \frac{h^\varrho}{\Gamma(\varrho+2)}(\theta {x^s_1}^p_{n+1} {x^i_1}^p_{n+1} - \varphi {x_2}^p_{n+1} {x^i_1}^p_{n+1} - d_1 {x^i_1}^p_{n+1}) \\
& + \frac{h^\varrho}{\Gamma(\varrho+2)} \sum_{j=0}^{n} \varpi_{j,n+1}(\theta x^s_{1j} x^i_{1j} - \varphi x_{2j} x^i_{1j} - d_1 x^i_{1j}), \\
x_{2n+1} =& x_2(0) + \frac{h^\varrho}{\Gamma(\varrho+2)}(\Omega {x^s_1}^p_{n+1} - \frac{\mu(1-m){x_2}^p_{n+1} y^p_{n+1}}{1 + a(1-m){x_2}^p_{n+1}} + \psi {x_2}^p_{n+1} {x^i_1}^p_{n+1} \\
& - \eta {x_2^2}^p_{n+1} - d_2 {x_2}^p_{n+1}) + \frac{h^\varrho}{\Gamma(\varrho+2)} \sum_{j=0}^{n} \varpi_{j,n+1}(\Omega x^s_{1j} - \frac{\mu(1-m)x_{2j}y_j}{1 + a(1-m)x_{2j}} \\
& + \psi x_{2j} x^i_{1j} - \eta x^2_{2j} - d_2 x_{2j}), \\
y_{n+1} =& y(0) + \frac{h^\varrho}{\Gamma(\varrho+2)}(\frac{\sigma(1-m){x_2}^p_{n+1} y^p_{n+1}}{1 + a(1-m){x_2}^p_{n+1}} - d_3 y^p_{n+1}) \\
& + \frac{h^\varrho}{\Gamma(\varrho+2)} \sum_{j=0}^{n} \varpi_{j,n+1}(\frac{\sigma(1-m)x_{2j}y_j}{1 + a(1-m)x_{2j}} - d_3 y_j),
\end{aligned}$$

where

$$\varpi_{j,n+1} = \begin{cases} n^{\varrho+1} - (n-\varrho)(n+1)^\varrho, & \text{if } j = 0, \\ (n-j+2)^{\varrho+1} + (n-j)^{\varrho+1} - 2(n-j+1)^{\varrho+1}, & \text{if } 0 \le j \le n, \\ 1, & \text{if } j = 1. \end{cases}$$

And the predictor formulae are

$$\begin{aligned}
{x^s_1}^p_{n+1} &= x^s_1(0) + \frac{1}{\Gamma(\varrho)} \sum_{j=0}^{n} \varepsilon_{j,n+1}(\alpha x_{2j} - \beta x^s_{1j} - \theta x^s_{1j} x^i_{1j}), \\
{x^i_1}^p_{n+1} &= x^i_1(0) + \frac{1}{\Gamma(\varrho)} \sum_{j=0}^{n} \varepsilon_{j,n+1}(\theta x^s_{1j} x^i_{1j} - \varphi x_{2j} x^i_{1j} - d_1 x^i_{1j}), \\
{x_2}^p_{n+1} &= x_2(0) + \frac{1}{\Gamma(\varrho)} \sum_{j=0}^{n} \varepsilon_{j,n+1}(\Omega x^s_{1j} - \frac{\mu(1-m)x_{2j}y_j}{1 + a(1-m)x_{2j}} + \psi x_{2j} x^i_{1j} - \eta x^2_{2j} - d_2 x_{2j})), \\
y^p_{n+1} &= y(0) + \frac{1}{\Gamma(\varrho)} \sum_{j=0}^{n} \varepsilon_{j,n+1}(\frac{\sigma(1-m)x_{2j}y_j}{1 + a(1-m)x_{2j}} - d_3 y_j),
\end{aligned}$$

where $\varepsilon_{j,n+1} = \frac{h^\varrho}{\varrho}((n+1-j)^\varrho - (n-j)^\varrho), 0 < j < n.$

References

1. Meyer, J.R.; Kassen, R. The effects of competition and predation on diversification in a model adaptive radiation. *Nature* **2007**, *446*, 432–435 [CrossRef] [PubMed]
2. Bohannan, B.J.M.; Lenski, R.E. The relative importance of competition and predation varies with productivity in a model community. *Am. Nat.* **2000**, *156*, 329–340. [CrossRef] [PubMed]
3. Kang, Y.; Wedekin, L. Dynamics of a intraguild predation model with generalist or specialist predator. *J. Math. Biol.* **2012**, *67*, 1227–1259. [CrossRef] [PubMed]
4. Barfield, M.; Holt, R.D.; Gomulkiewicz, R. Evolution in stage-structured populations. *Am. Nat.* **2011**, *177*, 397–409. [CrossRef] [PubMed]
5. de Valpine, P.; Scranton, K.; Knape, J.; Ram, K.; Mills, N.J. The importance of individual developmental variation in stage-structured population models. *Ecol. Lett.* **2014**, *17*, 1026–1038. [CrossRef]
6. eorgescu, P.; Hsieh, Y.-H. Global dynamics of a predator-prey model with stage structure for the predator. *SIAM J. Appl. Math.* **2007**, *67*, 1379–1395. [CrossRef]
7. Lu, Y.; Pawelek, K.A.; Liu, S. A stage-structured predator-prey model with predation over juvenile prey. *Appl. Math. Comput.* **2017**, *297*, 115–130. [CrossRef]
8. Oken, K.L.; Essington, T.E. How detectable is predation in stage-structured populations? Insights from a simulation-testing analysis. *J. Anim. Ecol.* **2015**, *84*, 60–70. [CrossRef]
9. Jalali, M.A.; Tirry, L.; De Clercq, P. Effect of temperature on the functional response of Adalia bipunctata to Myzus persicae. *BioControl* **2009**, *55*, 261–269. [CrossRef]
10. RRihan, F.A.; Lakshmanan, S.; Hashish, A.H.; Rakkiyappan, R.; Ahmed, E. Fractional-order delayed predator–prey systems with Holling type-II functional response. *Nonlinear Dyn.* **2015**, *80*, 777–789. [CrossRef]
11. Liu, Q.; Jiang, D.; Hayat, T.; Alsaedi, A. Dynamics of a stochastic predator–prey model with stage structure for predator and holling type II functional response. *J. Nonlinear Sci.* **2018**, *28*, 1151–1187. [CrossRef]
12. Zhang, H.; Cai, Y.; Fu, S.; Wang, W. Impact of the fear effect in a prey-predator model incorporating a prey refuge. *Appl. Math. Comput.* **2019**, *356*, 328–337. [CrossRef]
13. Liang, Z.; Meng, X. Stability and Hopf bifurcation of a multiple delayed predator-prey system with fear effect, prey refuge and Crowley-Martin function. *Chaos Solitons Fractals* **2023**, *175*, 113955. [CrossRef]
14. Tang, G.; Tang, S.; Cheke, R.A. Global analysis of a Holling type II predator–prey model with a constant prey refuge. *Nonlinear Dyn.* **2013**, *76*, 635–647. [CrossRef]
15. Wise, D.H. Cannibalism, food limitation, intraspecific competition, and the regulation of spider populations. *Annu. Rev. Entomol.* **2006**, *51*, 441–465. [CrossRef] [PubMed]
16. Claessen, D.; De Roos, A.M.; Persson, L. Population dynamic theory of size-dependent cannibalism. *Proc. R. Soc. London Ser. Biol. Sci.* **2004**, *271*, 333–340. [CrossRef] [PubMed]
17. Van Allen, B.G.; Dillemuth, F.P.; Flick, A.J.; Faldyn, M.J.; Clark, D.R.; Rudolf, V.H.W.; Elderd, B.D. Cannibalism and Infectious Disease: Friends or Foes? *Am. Nat.* **2017**, *190*, 299–312. [CrossRef] [PubMed]
18. Rosenheim, J.A.; Schreiber, S.J. Pathways to the density-dependent expression of cannibalism, and consequences for regulated population dynamics. *Ecology* **2022**, *103*, e3785. [CrossRef] [PubMed]
19. Posada-Florez, F.; Lamas, Z.S.; Hawthorne, D.J.; Chen, Y.; Evans, J.D.; Ryabov, E.V. Pupal cannibalism by worker honey bees contributes to the spread of deformed wing virus. *Sci. Rep.* **2021**, *11*, 8989. [CrossRef]
20. Li, J.; Zhu, X.; Lin, X.; Li, J. Impact of cannibalism on dynamics of a structured predator-prey system. *Appl. Math. Model.* **2020**, *78*, 1–19. [CrossRef]
21. Mishra, P.; Raw, S.; Tiwari, B. On a cannibalistic predator–prey model with prey defense and diffusion. *Appl. Math. Model.* **2020**, *90*, 165–190. [CrossRef]
22. Chen, M.; Fu, S. Global boundedness and stabilization in a predator-prey model with cannibalism and prey-evasion. *Electron. J. Qual. Theory Differ. Equ.* **2023**, *2023*, 1–23. [CrossRef]
23. Li, N.; Yan, M. Bifurcation control of a delayed fractional-order prey-predator model with cannibalism and disease. *Phys. A Stat. Mech. Its Appl.* **2022**, *600*, 127600. [CrossRef]
24. Biswas, S.; Samanta, S.; Chattopadhyay, J. Cannibalistic predator-prey model with disease in predator—A delay model. *Int. J. Bifurc. Chaos* **2015**, *25*, 1550130. [CrossRef]
25. Huang, C.; Song, X.; Fang, B.; Xiao, M.; Cao, J. Modeling, analysis and bifurcation control of a delayed fractional-order predator–prey model. *Int. J. Bifurc. Chaos* **2018**, *28*, 1850117. [CrossRef]
26. Zhang, F.; Chen, Y.; Li, J. Dynamical analysis of a stage-structured predator-prey model with cannibalism. *Math. Biosci.* **2018**, *307*, 33–41. [CrossRef] [PubMed]
27. Babakordi, N.; Zangeneh, H.R.Z. Multiple bifurcations analysis in a delayed predator-prey system with disease in prey and stage structure for predator. *Int. J. Dyn. Control* **2020**, *8*, 370–385. [CrossRef]
28. Tabouche, N.; Berhail, A.; Matar, M.M.; Alzabut, J.; Selvam, A.G.M.; Vignesh, D. Existence and stability analysis of solution for mathieu fractional differential equations with applications on some physical phenomena. *Iran. J. Sci. Technol. Trans. A Sci.* **2021**, *45*, 973–982. [CrossRef]

29. Jin, T.; Yang, X. Monotonicity theorem for the uncertain fractional differential equation and application to uncertain financial market. *Math. Comput. Simul.* **2021**, *190*, 203–221. [CrossRef]
30. Xu, C.; Aouiti, C.; Liu, Z.; Li, P.; Yao, L. Bifurcation caused by delay in a fractional-order coupled oregonator model in chemistry. *Match Commun. Math. Comput. Chem.* **2022**, *88*, 371–396. [CrossRef]
31. Yang, S.; Hu, C.; Yu, J.; Jiang, H. Exponential stability of fractional-order impulsive control systems with applications in synchronization. *IEEE Trans. Cybern.* **2019**, 50, 3157–3168. [CrossRef] [PubMed]
32. Gong, P.; Lan, W. Adaptive robust tracking control for multiple unknown fractional-order nonlinear systems. *IEEE Trans. Cybern.* **2018**, *49*, 1365–1376. [CrossRef] [PubMed]
33. Zhou, L.; Wang, S. The bright side of ecological stressors. *Trends Ecol. Evol.* **2023**, *38*, 568–578. [CrossRef]
34. Song, Y.; Wu, S.; Wang, H. Spatiotemporal dynamics in the single population model with memory-based diffusion and nonlocal effect. *J. Differ. Equ.* **2019**, *267*, 6316–6351. [CrossRef]
35. Xu, H. Analytical approximations for a population growth model with fractional order. Commun. *Nonlinear Sci. Numer. Simul.* **2009**, *14*, 1978–1983. [CrossRef]
36. Li, H.L.; Zhang, L.; Hu, C.; Jiang, Y.; Teng, Z. Dynamical analysis of a fractional-order predator-prey model incorporating a prey refuge. *J. Appl. Math. Comput.* **2017**, *54*, 435–449. [CrossRef]
37. Hasan, S.; El-Ajou, A.; Hadid, S.; Al-Smadi, M.; Momani, S. Atangana-Baleanu fractional framework of reproducing kernel technique in solving fractional population dynamics system. *Chaos Solitons Fractals* **2020**, *133*, 109624. [CrossRef]
38. Shi, J.; He, K.; Fang, H. Chaos, Hopf bifurcation and control of a fractional-order delay financial system. *Math. Comput. Simul.* **2021**, *194*, 348–364. [CrossRef]
39. Podlubny, I. *Fractional Differential Equations*; Academic Press: New York, NY, USA, 1999.
40. Li, K.; Peng, J. Laplace transform and fractional differential equations. *Appl. Math. Lett.* **2011**, *24*, 2019–2023.
41. Petras, I. *Fractional-Order Nonlinear Systems: Modeling Aanlysis and Simulation*; Higher Education Press: Beijing, China, 2011.
42. Liu, Q.; Zu, L.; Jiang, D. Dynamics of stochastic predator–prey models with Holling II functional response. *Commun. Nonlinear Sci. Numer. Simul.* **2016**, *37*, 62–76. [CrossRef]
43. Bhalekar, S.; Daftardar-Gejji, V. A predictor-corrector scheme for solving nonlinear delay differential equations of fractional order. *J. Fract. Calc. Appl.* **2011**, *1*, 1–9.